INITIAL NUMERICAL AND EXPERIMENTAL STUDIES TO DEVELOP A GROUND COUPLING RADAR FOR LOCATION AND IDENTIFICATION OF UNEXPLODED ARTILLERY SHELLS

Final Technical Report

Prepared by

Paul M. Goggans and Charles E. Smith

Department of Electrical Engineering
University of Mississippi

February 6, 1996

for

U. S. Army Research Office
Research Agreement No.
DAAH04-95-1-0403

Technical Report No. 96-1
Department of Electrical Engineering
University of Mississippi

Approved For Public Release; Distribution Unlimited

The views, opinions, and/or findings contained in this report are those of the authors and should not be construed as an official Department of the Army position, policy, or decision, unless so designated by other documentation.

REPORT DOCUMENTATION PAGE

Form Approved
OMB NO. 0704-0188

1. AGENCY USE ONLY *(Leave blank)*	2. REPORT DATE	3. REPORT TYPE AND DATES COVERED
	January 26, 1996	Final Technical Report

4. TITLE AND SUBTITLE
Initial Numerical and Experimental Studies to Develop a Ground Coupling Radar for Location and Identification of Unexploded Artillery Shells

5. FUNDING NUMBERS
DAAH04-95-1-0403

6. AUTHOR(S)
Paul M. Goggans and Charles E. Smith

7. PERFORMING ORGANIZATION NAMES(S) AND ADDRESS(ES)
Department of Electrical Engineering
University of Mississippi
University, MS 38677

8. PERFORMING ORGANIZATION REPORT NUMBER
UM 96-1 TR

9. SPONSORING / MONITORING AGENCY NAME(S) AND ADDRESS(ES)
U.S. Army Research Office
P.O. Box 12211
Research Triangle Park, NC 27709-2211

10. SPONSORING / MONITORING AGENCY REPORT NUMBER
ARO 34467.1-EL-II

11. SUPPLEMENTARY NOTES
The views, opinions and/or findings contained in this report are those of the author(s) and should not be construed as an official Department of the Army position, policy or decision, unless so designated by other documentation.

12a. DISTRIBUTION / AVAILABILITY STATEMENT
Approved for public release; distribution unlimited.

12 b. DISTRIBUTION CODE

13. ABSTRACT *(Maximum 200 words)*

Because of current efforts to clean former artillery ranges, there exists a need to develop an electromagnetic system to locate and identify subsurface artillery shells. Current ground penetrating radars are inadequate for the task because they are unable to couple sufficient energy into the ground without making an electrical connection to the earth. Here, we propose a ground coupling radar using an antenna with a predominately magnetic near field. The proposed radar will position the air-earth boundary in the near field of the antenna to couple energy into the ground. The proposed system depends on the enhanced coupling which occurs at the fundamental resonant frequency of the shell for detection and identification. Here we report on initial numerical and experimental studies to establish the feasibility of the ground coupling radar.

14. SUBJECT TERMS
Radar, Ground Coupled Radar, Detection of Buried Objects, Detection of Unexploded Shells

15. NUMBER IF PAGES

16. PRICE CODE

17. SECURITY CLASSIFICATION OR REPORT	18. SECURITY CLASSIFICATION OF THIS PAGE	19. SECURITY CLASSIFICATION OF ABSTRACT	20. LIMITATION OF ABSTRACT
UNCLASSIFIED	UNCLASSIFIED	UNCLASSIFIED	UL

Abstract

Because of current efforts to clean up former artillery ranges, there exists a need to develop an electromagnetic system to locate and identify subsurface artillery shells. Current ground penetrating radars are inadequate for the task because they are unable to couple sufficient energy into the ground without making an electrical connection to the earth. Here, we propose a ground coupling radar using an antenna with a predominately magnetic near field. The proposed radar will position the air-earth boundary in the near field of the antenna to couple energy into the ground. The proposed system depends on the enhanced coupling which occurs at the fundamental resonant frequency of the shell for detection and identification. Here we report on initial numerical and experimental studies to establish the feasibility of the ground coupling radar.

Acknowledgment

The Numerical Electromagnetics Computation program version 4 (NEC-4) was used to compute the antenna response when the antenna and target are in a free space region. The NEC-4 computer program was developed by the Lawrence Livermore National Laboratory.

The computer program used to compute the antenna response when the target is buried in a multilayer medium was developed by Dr. Weiping Zheng using a numerical Green's function calculation technique originated by Mr. Jangyang Chen and Dr. Ahmed Kishk.

Table of Contents

List of Figures

Introduction

The location and identification of buried unexploded artillery shells is a subject of great current interest because of the mandate to remove shells from former artillery ranges. Range clean up (which includes the removal of shells) is a very complex problem that will require a number of techniques to address. In the work proposed here, we narrow the focus of the problem to detecting and roughly identifying some specific types of targets using ground coupling (ground penetrating) radar.

Years of relatively fruitless research in the area of mine detection demonstrate the complexity of the buried anomaly detection problem. Fortunately, range clean up with ground penetrating radar is a more tractable problem than mine detection. This is because the constraints for range clean up are not as severe as those for mine detection. In range clean up work, one can wait until soil conditions are favorable to make measurements, can take as much time as necessary to obtain the data, and can process the measured data off line. These luxuries are out of the question on the battlefield. More important, one can use measurement equipment that would be impractical in battlefield conditions (such as antennas suspended from hovering aircraft).

A serious problem in ground penetrating radars is getting the incident energy into the ground and getting the energy scattered by the target back out of the ground. Antennas which are electrically distant from the ground produce a wave which is approximately plane at the ground. A plane wave incident onto the ground is mainly reflected from the ground because the impedance of the ground is low. The low impedance of the ground is due both to its high dielectric constant and its high conductivity. The ground reflection problem is further compounded because the energy scattered by the target is again mainly reflected from the ground air boundary. Another problem associated with the conductivity of the earth is the attenuation that the electromagnetic wave experiences when propagating through the earth. To be useful, a new ground penetrating radar must be designed to mitigate these problems.

A Ground Coupling Radar System

Because the attenuation per meter is proportional to the square root of the operating frequency, choice of a low operating frequency tends to mitigate the problem of electromagnetic wave attenuation in the ground. Here we propose to use a CW radar which slowly scans a band of frequencies in the vicinity of the fundamental resonant frequency of each type of unexploded shell in the former artillery range. Because the shells have enhanced coupling with the antenna at their resonant frequencies, this technique can be used to detect the shell by sensing the enhanced coupling at the resonant frequency. Shells are axisymmetric bodies with relatively high length to maximum diameter ratios. The fundamental resonance frequency of a shell can be determined from the length of its generating curve. The resonant frequency is approximately the frequency at which the length of the generating curve is one-half of a wavelength. Because the fundamental resonance occurs at a frequency related to the dimension and shape of the shell this technique allows for identification based on shell size.

Using a low frequency also helps mitigate the ground/air boundary reflection problem. If the antenna is less than around a wavelength from the boundary, the wave impedance at the boundary is not the characteristic impedance of air as it is for a plane wave, but rather is determined by the characteristics of the antenna (the actual near field region also has to do with the antenna size). Loop antennas have a larger proportion of magnetic field than electric field (relative to a plane wave) in the near field region so that the wave impedance in the near field region is less than the characteristic impedance of air. By placing the boundary in the near field region of a loop antenna, the impedance of the wave can be more nearly matched to the impedance of the ground, thus reducing the reflection of the incident wave. Because of reciprocity, this technique also reduces the reflection of the wave scattered from the shell. For the frequencies proposed here, an antenna suspended from a helicopter could be positioned so that the ground is in the near field region.

The position of detected shells would be determined from the position of the antenna when detection occurs. These measurements are relatively crude, but should be sufficient for the purpose of removing the shell. Determining the depth of the shell is more problematic since the proposed radar is CW. The range to the target will have to be determined from some indirect measure, such as, the amount of coupling between the antenna and the shell.

The identification of subsurface targets using resonant frequencies has been established experimentally by Chan, Moffatt and Peters [1]. In this work, a broadband signal was broadcast and poles of the buried target were extracted from the return signal and used for identification. Note that the radar used in this experiment is not appropriate for range clean up because its antenna requires direct connection to the ground. For range clean up applications, we believe that only the antenna-target coupling (for example, measured by the change in the antenna input admittance) in the frequency range about the resonant frequency of the lowest frequency pole can be used for identifying unexploded shells. An identification method based on a single mode (pole) enhancement pulse is discussed in [2]. In this technique, an enhancement pulse for each target to be located is transmitted at each location of interest. Single mode enhancement pulses are referred to as the T-pulses. A related identification method based on extracting the resonant frequency and Q factor of the lowest frequency pole from target returns is described in [3, 4]. In this technique, a broad band signal pulse is transmitted from an antenna placed on the surface of the earth. The technique proposed here is different from the single mode extraction method and the T-pulse method because it uses the enhanced coupling that occurs between a magnetic field antenna and the shell at frequencies around the shell's resonant frequency for detection (using a CW radar) rather than a pulse. Identification based on coupling at the shell's fundamental resonant frequencies is also attractive for range clean up because it mitigates the problem of clutter return from exploded shell fragments. Fragments should be much smaller than unexploded shells and so have much higher fundamental resonant frequencies.

Summary of Results

Figure 1 illustrates the antenna and target geometry considered here. The antenna is a gap-driven loop of radius r_a and wire thickness (diameter) t_a. The center of the antenna loop is in free space a distance D_a from a planer free-space/soil boundary. The target is treated as a linear wire segment of length L and wire thickness t_s. The wire target is parallel to the free-space/soil boundary. The loop antenna and the wire target are in the same plane and the center of the antenna loop is separated from the center of the wire target by the distance D. The distance from the free-space/soil boundary to the center of the wire target is D_s.

We had initially proposed to model the target using a wire loop tuned with a lumped capacitor. Upon reflection, we changed to a linear wire model because it better represents the actual coupling between a shell and the antenna and because the induced currents on the wire model better represent the surface currents on an actual shell.

In the numerical work, the antenna is driven by a unity valued ideal voltage source. The quantity we observe in the numerical work is the antenna input admittance Y. Because we use a unity valued voltage source, the antenna input admittance is numerically equal to the antenna terminal input current.

The measured data was obtained using a microwave network analyzer. The analyzer is set up to measure the voltage reflection coefficient at the antenna terminals (denoted as Γ or S_{11}). The input admittance can be determined from the reflection coefficient and vice versa. For example, to calculate the input admittance from the reflection coefficient the following expression is used: $Y = Y_o(1+\Gamma)/(1-\Gamma)$ where Y_o is the characteristic admittance of the transmission line connected to the antenna.

Numerical

For the purpose of calculating the loop antenna input admittance when both the antenna and target are in free space, Version 4 of the Numerical Electromagnetic Code (NEC-4) developed at Lawrence Livermore National Laboratory was used [5]. NEC-4

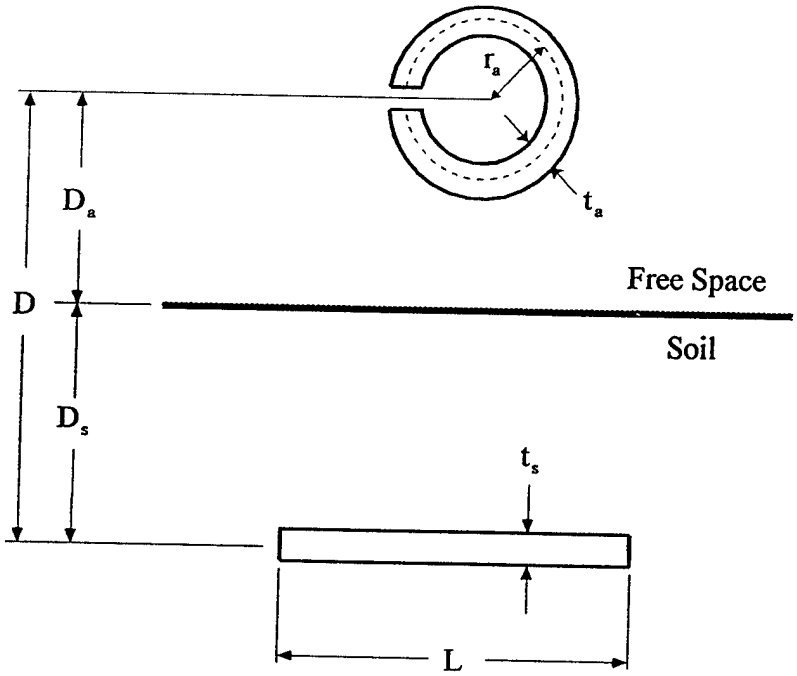

Figure 1. Illustration of the loop antenna and the wire target.

uses a numerical solution method (the moment method) to solve the electric field integral equation for the currents on a wire antenna due to a voltage source on the antenna.

When calculating the loop antenna input admittance with the antenna in free space and the target in soil, a computational electromagnetics (CEM) program under development at the University of Mississippi was used. Like NEC-4, the CEM program uses a numerical solution method (the moment method) to solve the electric field integral equation for the currents on a wire antenna due to a voltage source on the antenna. Because the program treats multilayer medium, a numerical Green's function is used in the generation of the moment method impedance elements. The method used to calculate the numerical Green's function was developed by Mr. Jangyang Chen and Dr. Ahmed Kishk [6]. The actual development and testing of the program used in this work was performed by Dr. Weiping Zheng [7, 8]. As part of the work reported here, the CEM program was modified by Mr. Wenhai Yang to include the effect of a lumped impedance located in the wire antenna or wire target.

A uniform antenna and target geometry was used to generate data presented in the numerical results section. The parameter values which define this geometry are as follows: $r_a = 3$ cm, $t_a = 158.75$ mm ($\frac{1}{16}$ inch), L = 60 cm, and $t_s = 317.50$ mm ($\frac{1}{8}$ inch).

Figure 2 is a plot of the induced current on the wire target for a frequency near the fundamental resonant frequency of the wire target and for frequencies above and below the fundamental resonant frequency. This figure illustrates the physical mechanism which causes the enhanced coupling between the target and the antenna at the fundamental resonant frequency of the target. Readers familiar with antenna theory will observe that the current distribution for 220 MHz is the same as that on a one-half wavelength dipole antenna. Enhanced coupling occurs at resonance because of the increased current on the target at the resonant frequency compared to the current at other frequencies. The antenna current distributions around the antenna loop for the same frequencies used for Fig. 2 are plotted in Fig. 3. The current minimum at 9.4 cm on the distance around the loop scale corresponds to the position of the antenna terminals. In general, the magnitude of the current on the antenna decreases with increasing operating frequency. This is because the

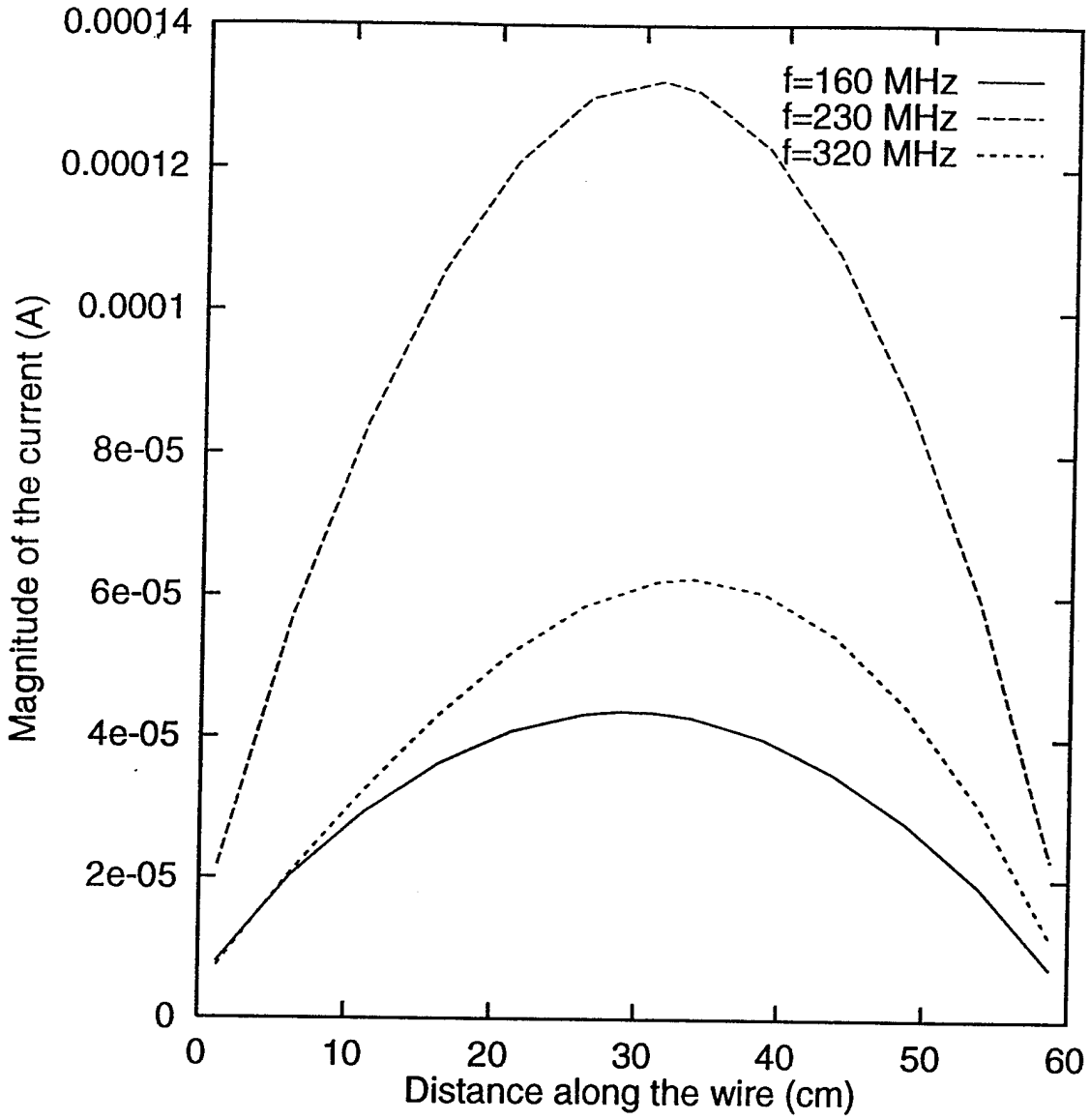

Figure 2. Magnitude of the current on a wire target versus distance around the loop for a loop antenna in the presence of a wire target with center 40 cm from the loop center.

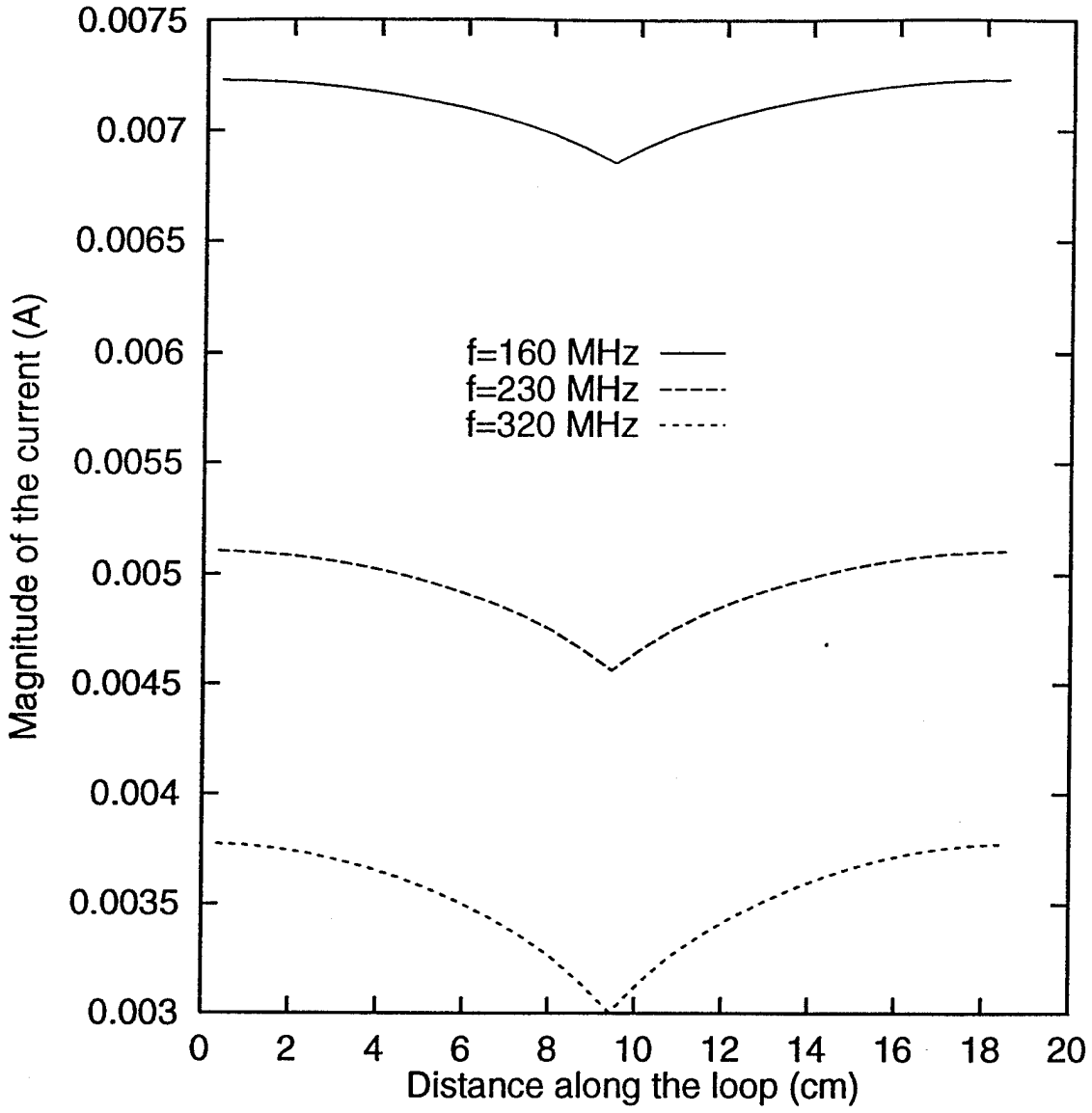

Figure 3. Magnitude of the current on the loop versus distance around the loop for a loop antenna in the presence of a wire target with center 40 cm from the loop center.

magnitude of the input admittance of the isolated loop antenna is a decreasing function of frequency. The decreasing magnitude of the input admittance is illustrated in Figs. 4 and 5, which are plots of the real and imaginary parts of the antenna input admittance, respectively.

In Figs. 4 and 5, admittance results are given for the antenna alone and for the antenna with the wire target present. In Fig. 4, the effect of the target on the antenna input conductance is clearly visible. In Fig. 5, the effect of the target on the antenna input susceptance is not visible. Figures 2 through 5 are for a target depth of 40 cm (D = 40 cm). Figure 6 is a plot of the antenna input conductance versus frequency for a target depth of 160 cm. As in Fig. 4, the effect of the target is visible when comparing the conductance values for the cases with and without the target present.

One method of observing the increased coupling from measurements or calculations made at the antenna terminals is to plot one minus the magnitude of the ratio of the terminal admittance with the target present, Y, to the terminal admittance of the isolated antenna, Y_i. We refer to this quantity as the target sensing function, T_s. The target sensing function is written symbolically as $T_s = 1 - |Y/Y_i|$. In the absence of a target, the admittance ratio is one for all frequencies so that one minus the magnitude of the admittance ratio is zero. Therefore, when no target is present, the target sensing function is zero. With the target present, the quantity one minus the magnitude of the admittance ratio exhibits a minimum or maximum at a frequency close to the target's resonant frequency for target depths in the near field region of the loop antenna. Figures 7 though 9 demonstrate this for a wire target at a distance of 40 cm, 80 cm, and 160 cm from the center of the antenna. Results in Fig. 7 though 9 are for the antenna and target in free space. In Fig. 9 (for D = 160 cm), the target is no longer in the near field of the antenna and although the presence of the target is clearly visible, there is no peak or null in the $1 - |Y/Y_i|$ data near the target's resonant frequency.

The loop antenna with radius $r_a = 3$ cm is resonant at approximately 1.6 GHz. At frequencies in the vicinity of the target's fundamental resonant frequency, the antenna has a small radiation resistance and is primarily inductive. The sensitivity of the ground

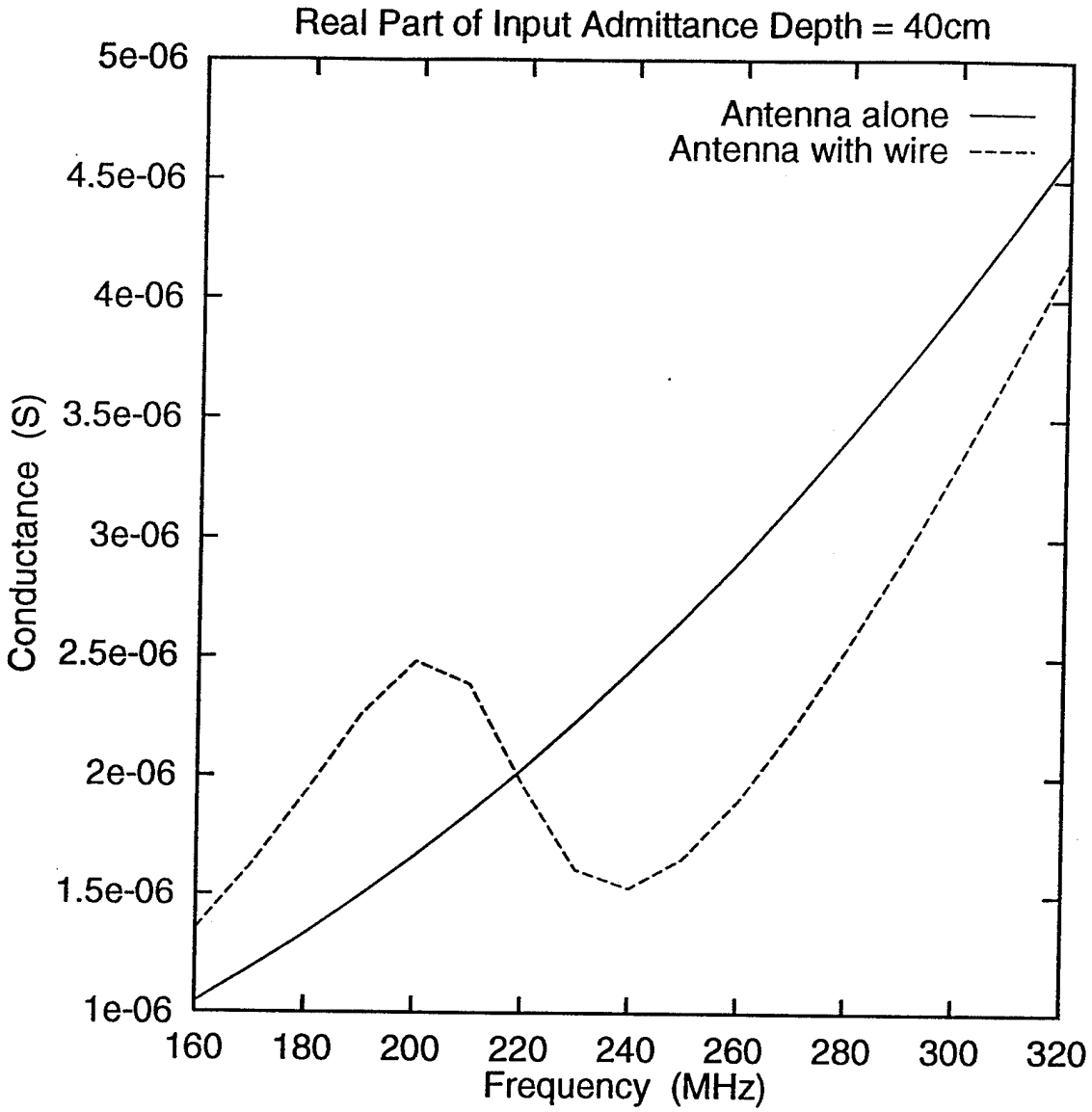

Figure 4. Input conductance of the loop antenna versus frequency with and without a wire target with center 40 cm from the loop center.

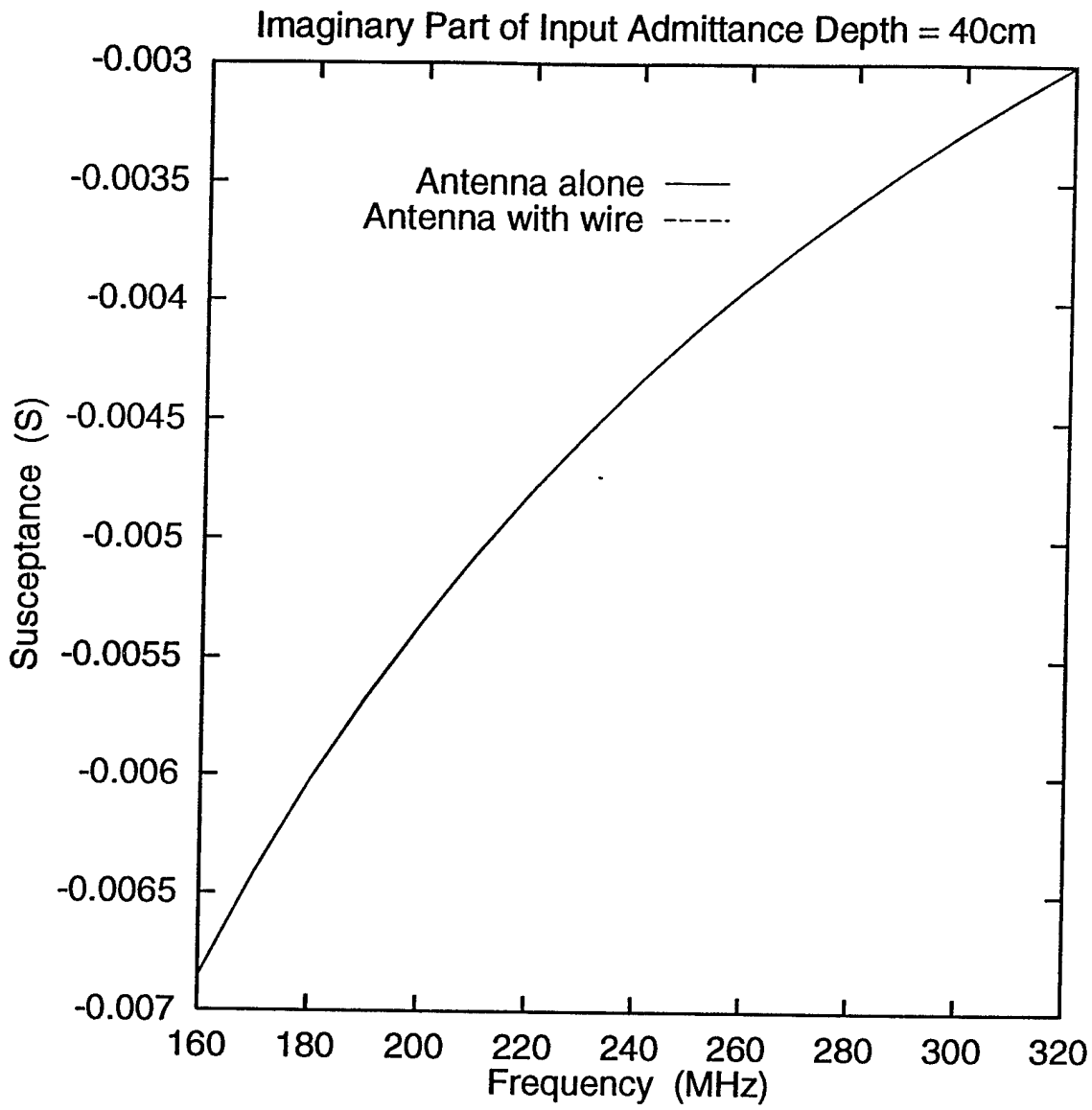

Figure 5. Input susceptance of the loop antenna versus frequency with and without a wire target with center 40 cm from the loop center.

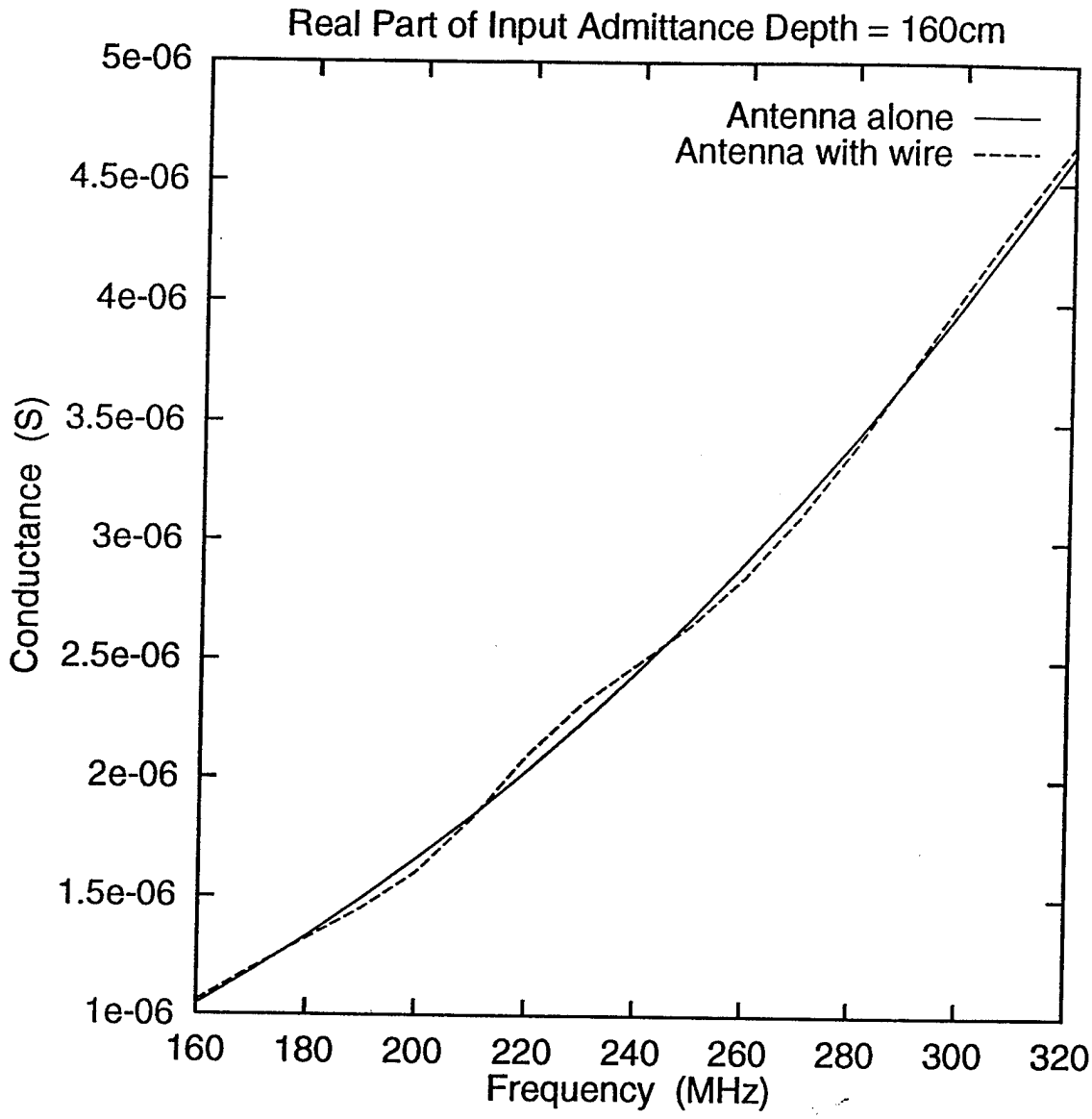

Figure 6. Input conductance of the loop antenna versus frequency with and without a wire target with center 160 cm from the loop center.

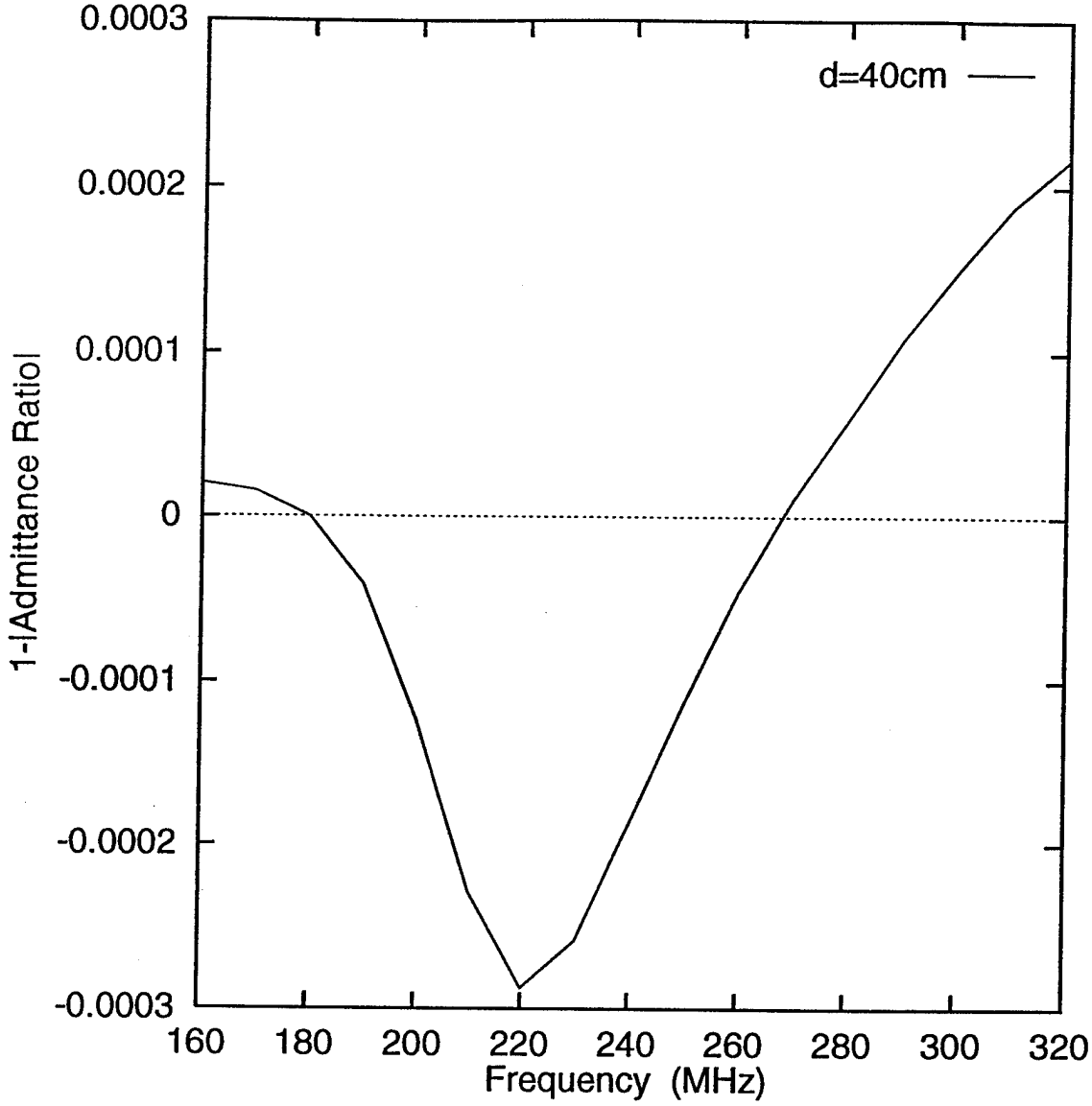

Figure 7. One minus the magnitude of the ratio of the loop antenna input admittance with a target present to the input admittance of the isolated loop versus frequency. The center of the wire target is 40 cm from the center of the loop.

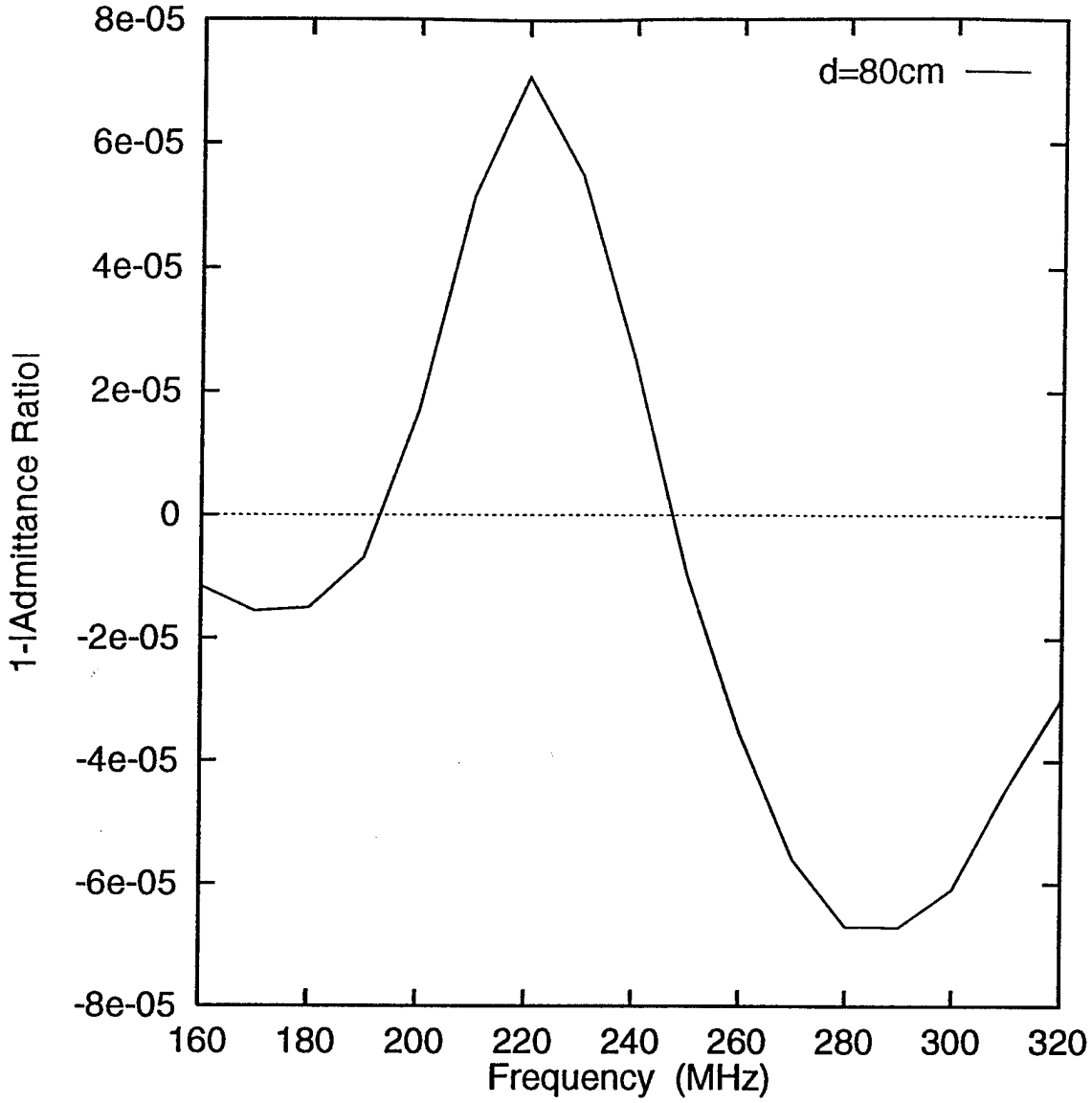

Figure 8. One minus the magnitude of the ratio of the loop antenna input admittance with a target present to the input admittance of the isolated loop versus frequency. The center of the wire target is 80 cm from the center of the loop.

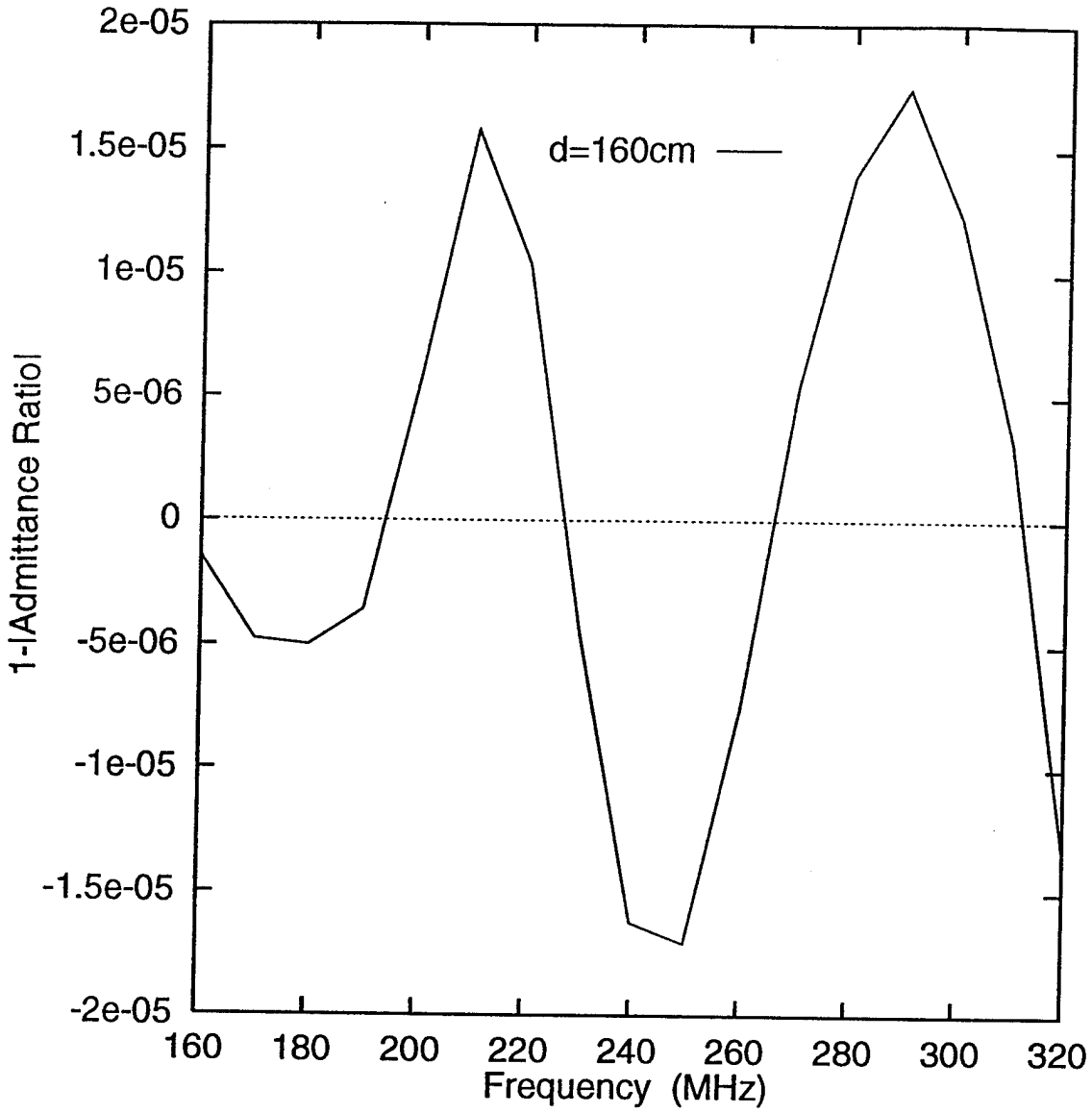

Figure 9. One minus the magnitude of the ratio of the loop antenna input admittance with a target present to the input admittance of the isolated loop versus frequency. The center of the wire target is 160 cm from the center of the loop.

coupling radar system can be greatly increased by adding a capacitor to the loop antenna to tune the loop to resonance at the measurement frequency. Figure 10 demonstrates the increase in sensitivity achievable using this method. In Fig. 10, the target is at D = 160 cm and a capacitor is added to the loop antenna in the zone next to the zone containing the terminals. At each frequency, the capacitor value is set so that the input impedance of the isolated antenna is entirely real. The increase in sensitivity of the tuned system is apparent when Fig. 10 is compared to Fig. 8.

The shape of the response curve in Fig. 10 can be understood by considering a simple circuit model for the antenna and target interaction. In this model the antenna is a series resonant circuit composed of a resistor, a capacitor and an inductor. The target is modeled as a parallel resonant circuit again composed of a resistor, a capacitor, and an inductor. The coupling between the antenna and target is modeled by a mutual inductance between the inductor in the antenna circuit and the inductor in the target circuit. The mutual inductance is much less than the self inductance of the antenna and much less than the self inductance of the target. The Q of the target is low (less than five) and the resonant frequency is the fundamental resonant frequency of the target. Because of the low radiation resistance of the antenna, the Q of the antenna circuit model is very large (it is a very narrow band system). The shape of the target sensing function versus frequency curve in Fig. 10 is the expected result when the resonant frequency of a high Q resonant circuit which is loosely coupled to a low Q system is scanned through the resonant frequency of the low Q system.

Figures 11 and 12 are plots of target sensing function for the antenna tuned to the fixed frequencies of 230 MHz and 250 MHz. These figures demonstrate that the tuned antenna is a very narrow bandwidth (high Q) system.

The orientation of the wire target with respect to the horizontal plane has a marked effect on the response of the system. This effect is demonstrated in Fig. 13 which plots $1-|Y/Y_i|$ versus the angle the wire antenna makes with the horizontal plane. As expected, the presence of the target cannot be detected when the target is perpendicular to the horizontal plane.

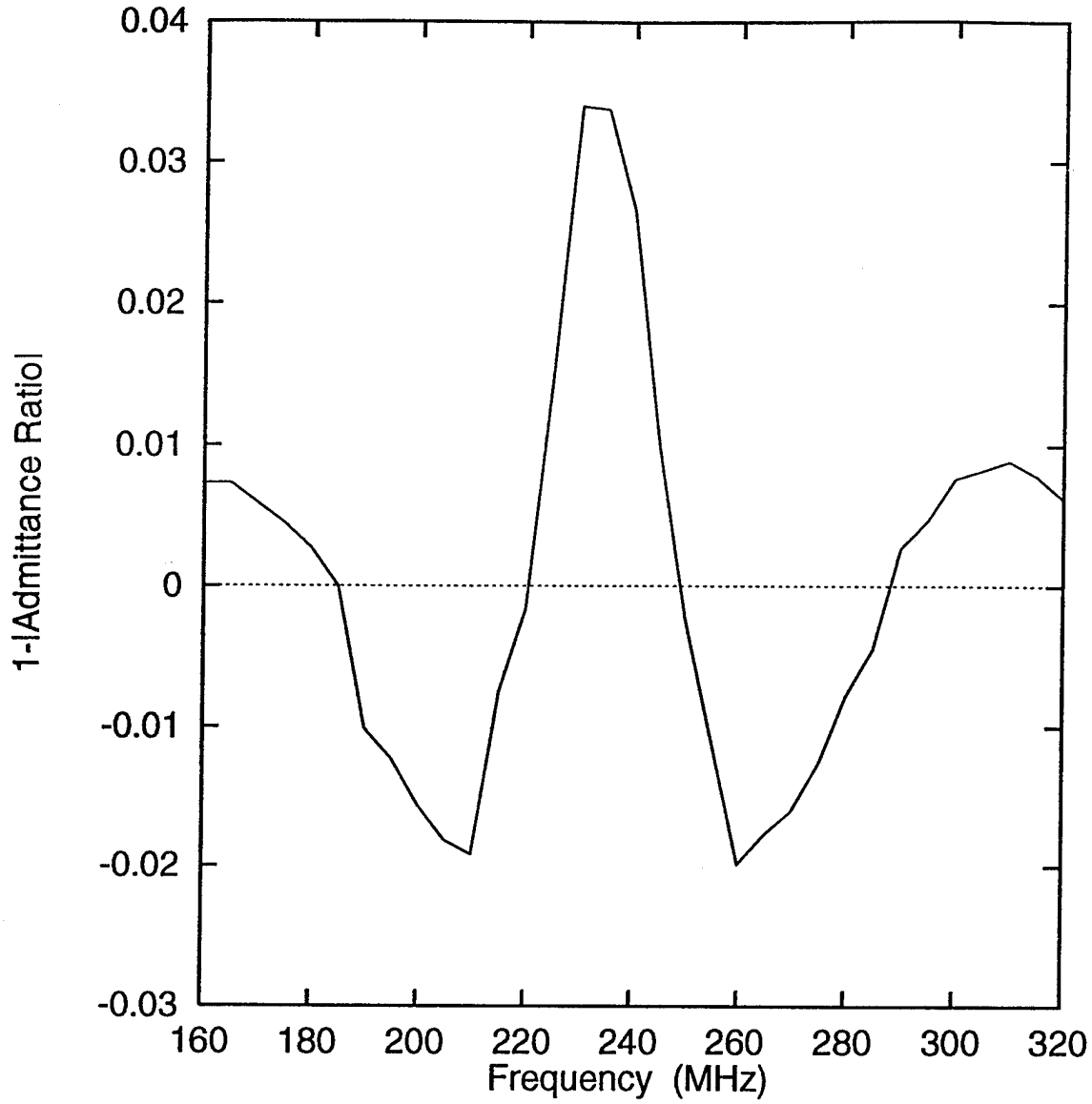

Figure 10. One minus the magnitude of the ratio of the loop antenna input admittance with a target present to the input admittance of the isolated loop versus frequency. The center of the wire target is 160 cm from the center of the loop and the loop is capacitively tuned to the measurement frequency.

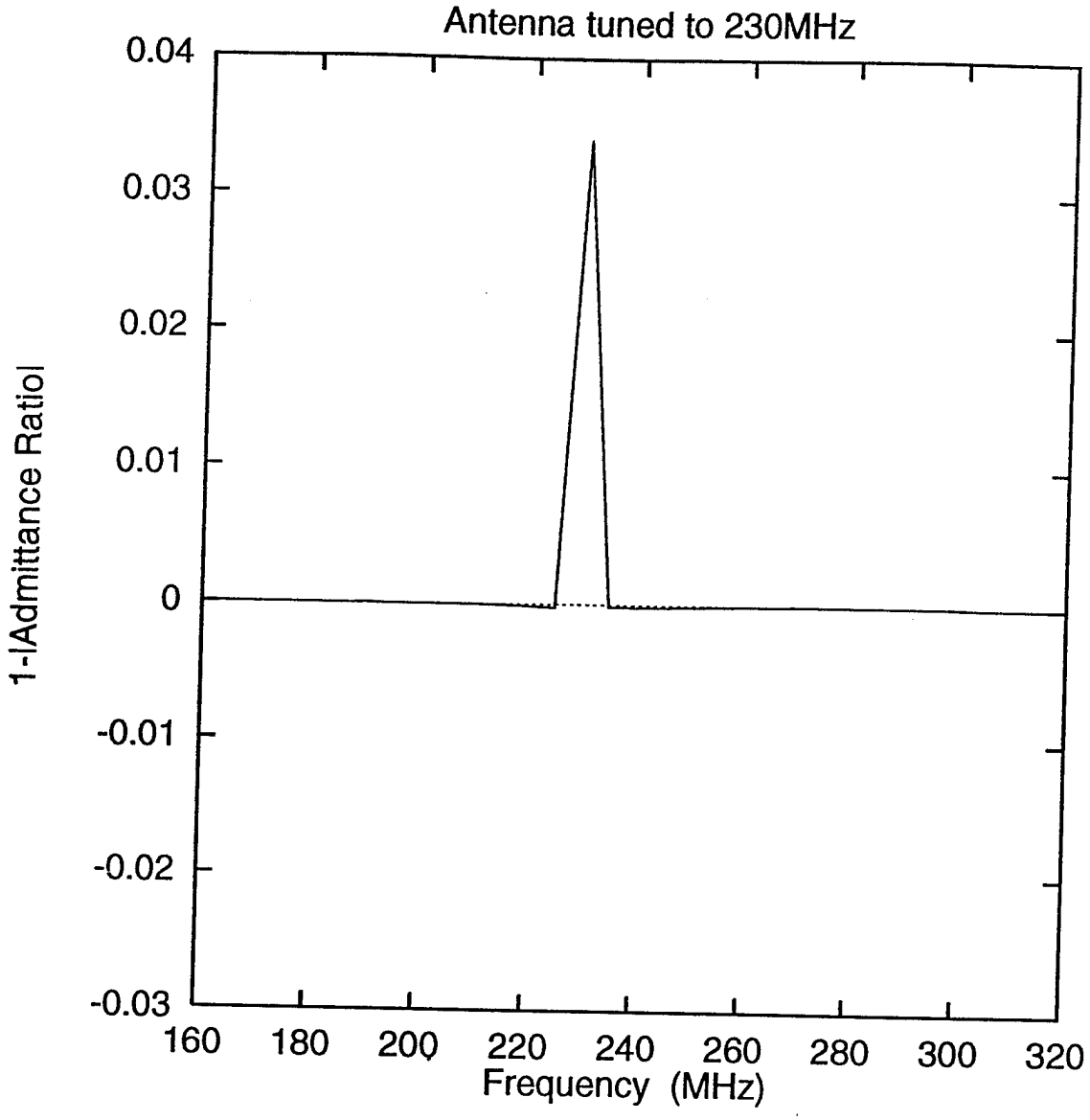

Figure 11. One minus the magnitude of the ratio of the loop antenna input admittance with a target present to the input admittance of the isolated loop versus frequency. The center of the wire target is 160 cm from the center of the loop and the loop is capacitively tuned to 230 MHz.

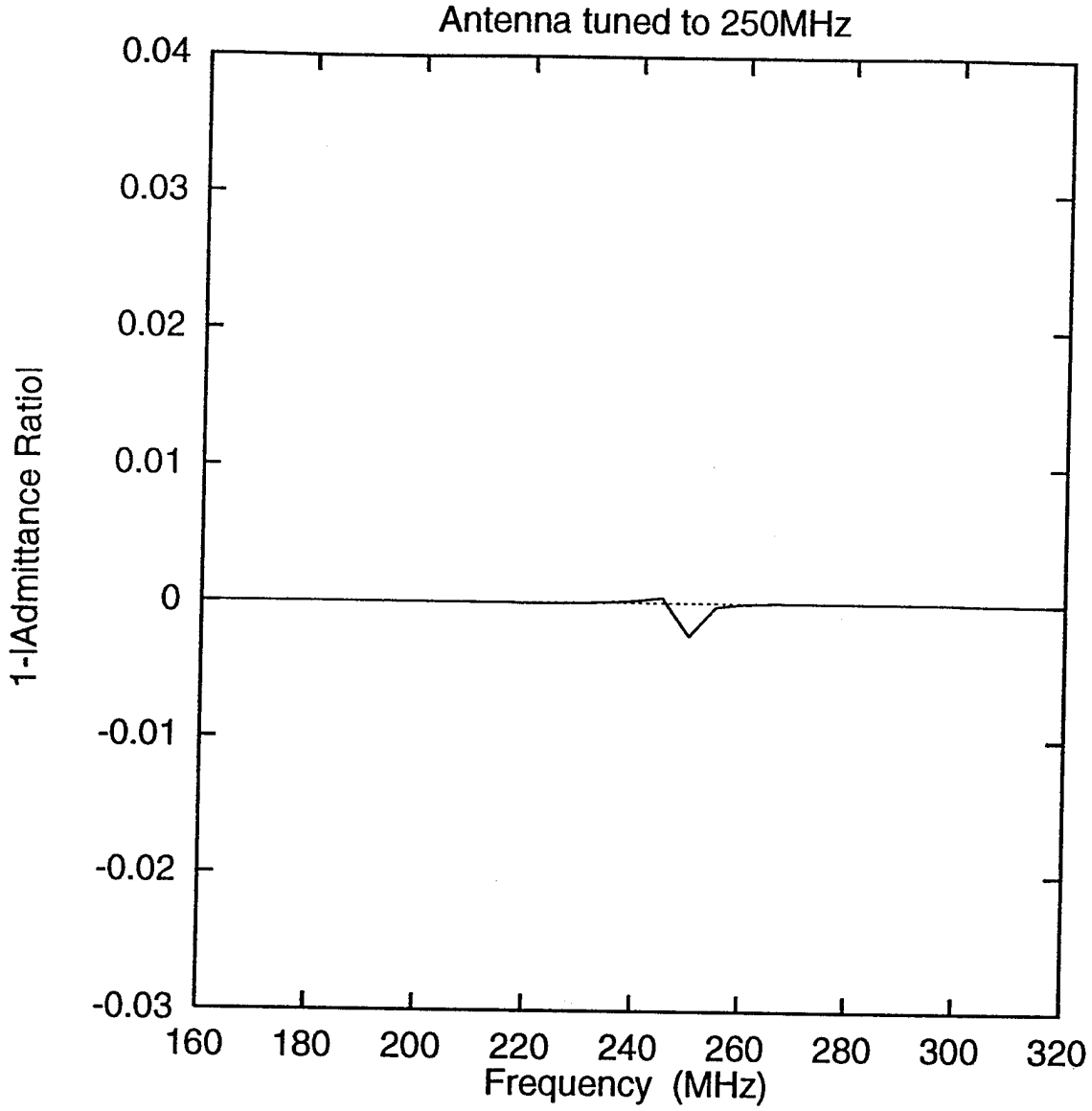

Figure 12. One minus the magnitude of the ratio of the loop antenna input admittance with a target present to the input admittance of the isolated loop versus frequency. The center of the wire target is 160 cm from the center of the loop and the loop is capacitively tuned to 250 MHz.

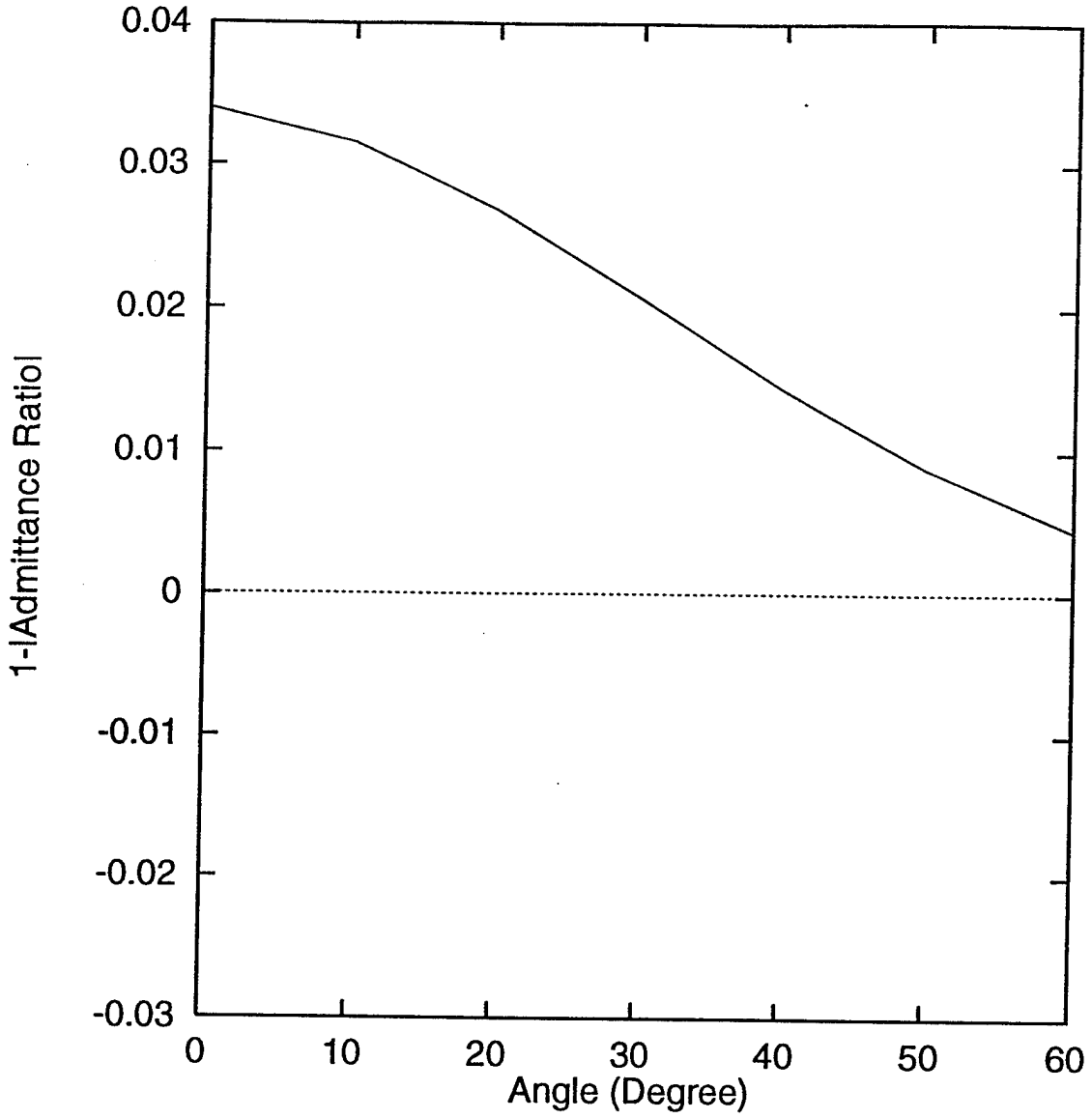

Figure 13. One minus the magnitude of the ratio of the loop antenna input admittance with a target present to the input admittance of the isolated loop versus angular deviation of the wire from tangent to the loop. The center of the wire target is 160 cm from the center of the loop and the loop is capacitively tuned to the 230 MHz excitation frequency.

Introduction of lossy soil greatly effects the behavior of the loop antenna and wire target system. In Fig. 14, the target sensing function is plotted versus frequency for an untuned antenna loop. For Fig. 14, the target is in a lossy soil a distance of 60 cm from the free-space/soil boundary ($D_2 = 60$ cm) and the center of the loop antenna is 20 cm above the free-space/soil boundary ($D_1 = 20$ cm). The soil is treated as lossy dielectric with $\varepsilon_r' = 2.6$ and $\varepsilon_r'' = 0.30$. The wavelength in the lossy soil is 80.7 cm at 230 MHz. In free space, the wavelength at 230 MHz is 130 cm. So that the target's resonant frequency in the soil is approximately the same as in the previous figures, the target length, L, was changed to 40 cm for these calculations. Comparing Fig. 14 and Fig. 8 demonstrates the effect the soil has on the target sensing function. As noted above, the lossy soil lowers the target's fundamental resonant frequency because the wavelength in the soil is less than the wavelength in free space. This effect is partially compensated for in Fig. 14 by shortening the target length (compared to the target length used for Fig. 8). The Q on the target is also reduced by the soil loss. This effect can be seen by comparing the width of the dip around the resonant frequency in Figs. 8 and 14. The peak deviation in the target sensing function in Fig. 14 is reduced by a factor of around one half compared to Fig. 14. Some of this reduction may due to the shorter length of the target used for Fig. 14. The numerical results, which include the lossy ground (such as Fig. 14), indicate that use of an antenna with a primarily magnetic near field is effective in coupling energy into the ground.

Measured

Measurements were performed to gain insight into the measurement and hardware issues related to the proposed technique for sensing unexploded artillery shells. In addition, measurements were performed to validate both the measurement technique used here and the numerical solutions presented in the previous section.

To physically represent the basic loop-target configuration for measurement purposes, a simulated half-plane environment was used. This measurement region consisted of a 5 foot by 6 foot ground plane with a centered mounted half loop antenna. Surrounding anechoic material was used as required. Figure 15 diagrams the experimental

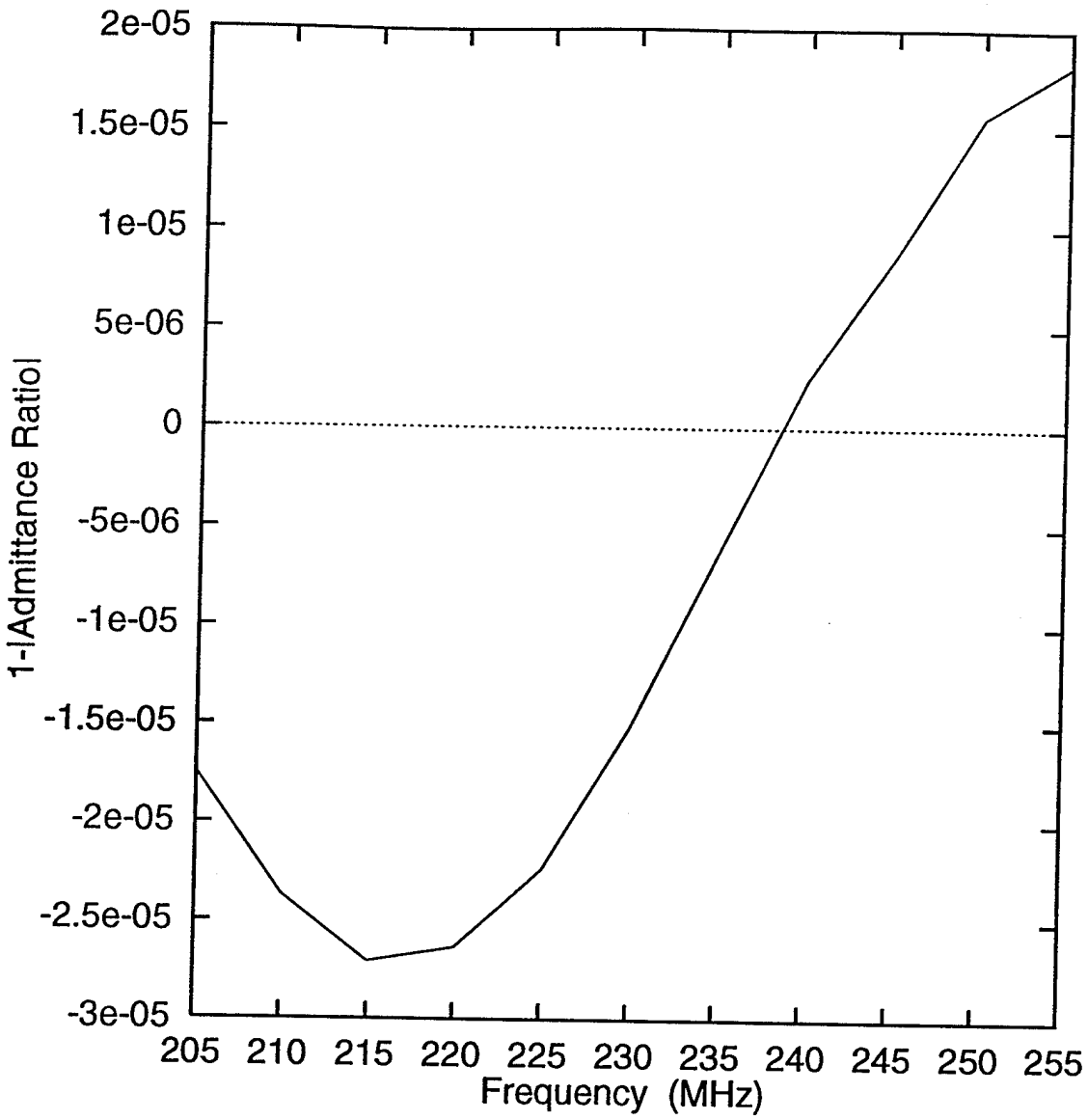

Figure 14. One minus the magnitude of the ratio of the loop antenna input admittance with a target present to the input admittance of the isolated loop versus frequency. The center of the wire target is 80 cm from the center of the loop. The center of the loop is in air 20 cm from a planer material boundary. The material is lossy dielectric with $\varepsilon_r' = 2.6$ and $\varepsilon_r'' = 0.30$. The loop antenna is untuned. The wire target is buried in the lossy dielectric 60 cm below the material boundary. The length of the wire target is 40 cm.

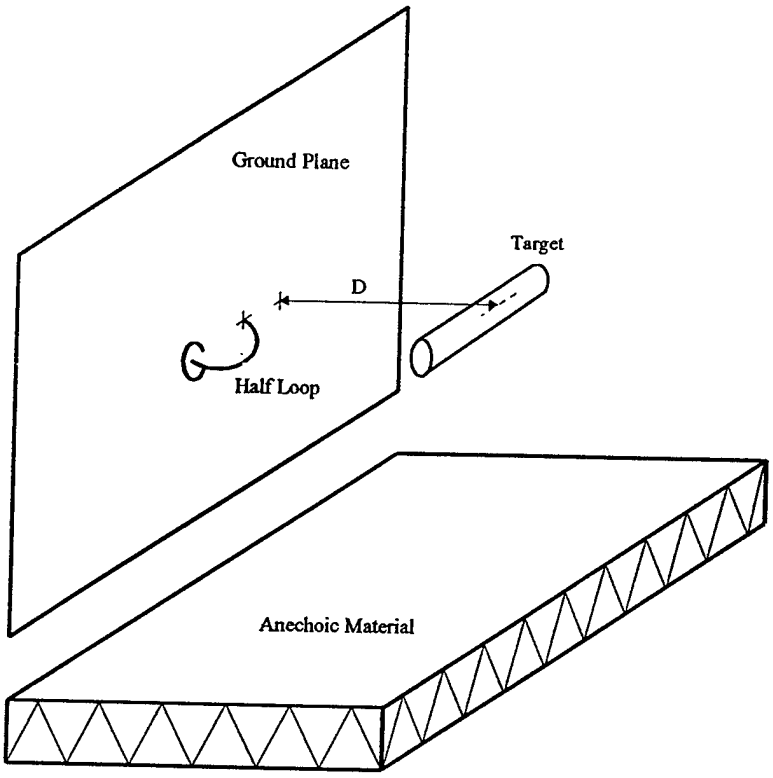

Figure 15. Ground plane modeling of loop-target configuration.

setup. For the measurements, the loop antenna has a radius r_a = 3.25 cm and is constructed from a curved brass rod of thickness t_a = 0.635 cm (¼"). Two targets were used for the measurements. Both targets are 56 cm in length. The thickness, t_s, of the two targets are 0.635 cm and 1.829 cm. A relatively small ground plane was used because the near field of the loop is of primary interest. The range of frequencies used for measurements was from 200 to 300 MHz with smaller subsets of this frequency range used for specific geometries. The fundamental resonant frequency of the measurement targets were near mid-band (250 MHz). The mid-band frequency was selected as the primary measurement frequency. Note that because these measurements were made with an image plane, comparisons with numerical models must account for both the image of the loop and the image of the target.

Measurements of the scattering parameter, S_{11} (reflection coefficient, Γ) were made, using the loop-configuration of Fig. 15, for different target separation distances, D. The measurements were made using a Hewlett Packard HP8510B Vector Network Analyzer (VNA) employing either response calibration or the 3-standard calibration (short-open-load) for S_{11} measurements. With this setup, two basic configurations were studied:

1. An untuned loop (using 3-standard calibration), and
2. A single stub tuned loop (using response calibration).

A set of measurements of the untuned loop were made using the configuration given in Fig. 15 and the HP8510B network analyzer for target distances of D = 8, 10, 15, 20, 25, and 40 cm using the 56 cm targets. The measured data, consisting of the real and imaginary part of S_{11} (Γ), are presented in Figs. 16 through 19. The target used for Figs. 16 through 19 was the 0.635 cm thickness rod. As can be seen from the figures, the coupling between the loop and target becomes very small with increasing distance, and the results for the no target (NT) case essentially falls on top of the results for a target distance of 40 cm. The same untuned loop configuration was used to measure target coupling for a target of the larger thickness rod (1.829 cm) and the results of these measurements are given in Figs. 20 and 21. This data shows that a thicker target has a

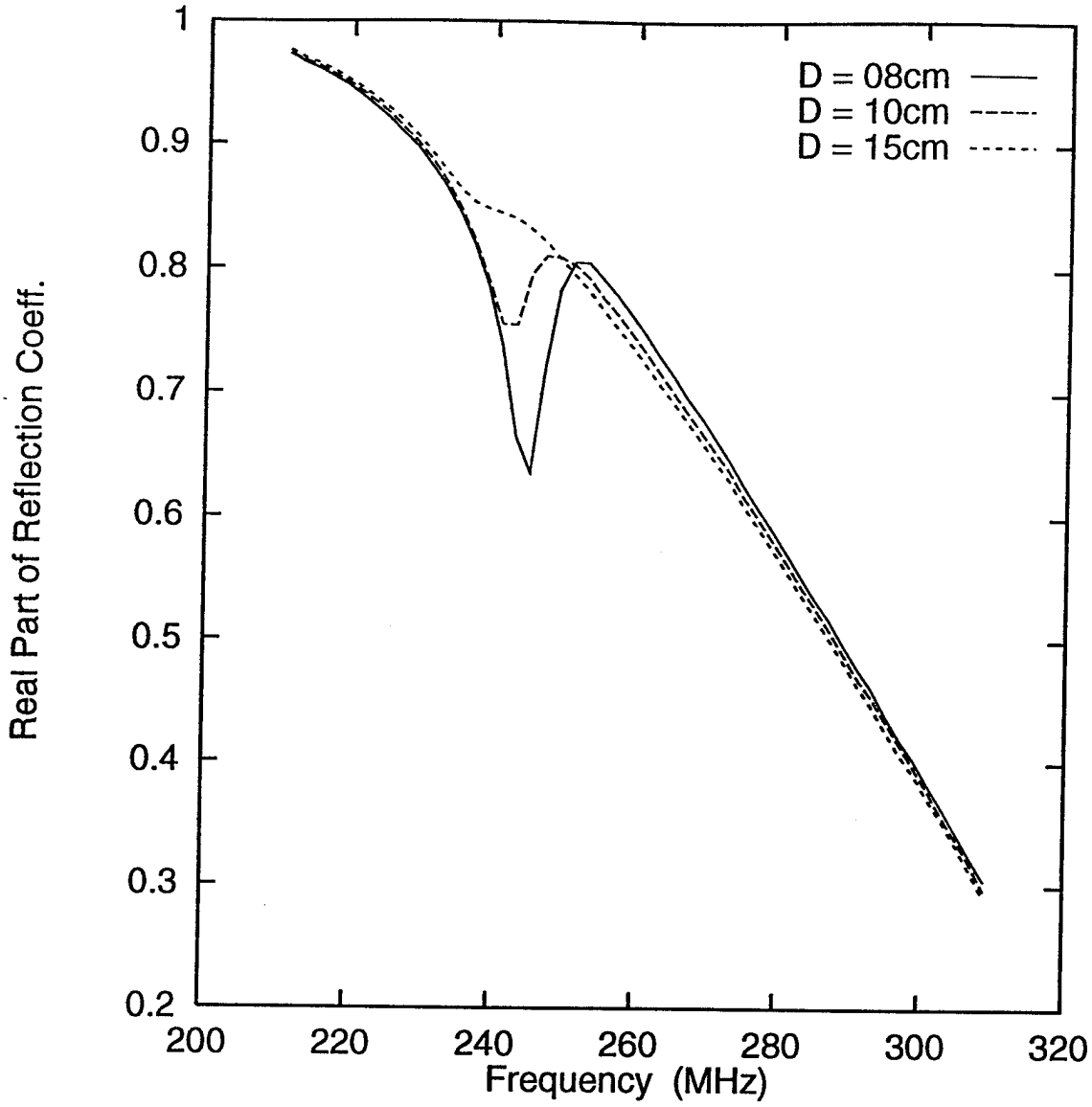

Figure 16. Real part of S_{11} (Γ) for an untuned loop and target distances of D = 8,10, and 15 cm for a 0.635 cm target thickness.

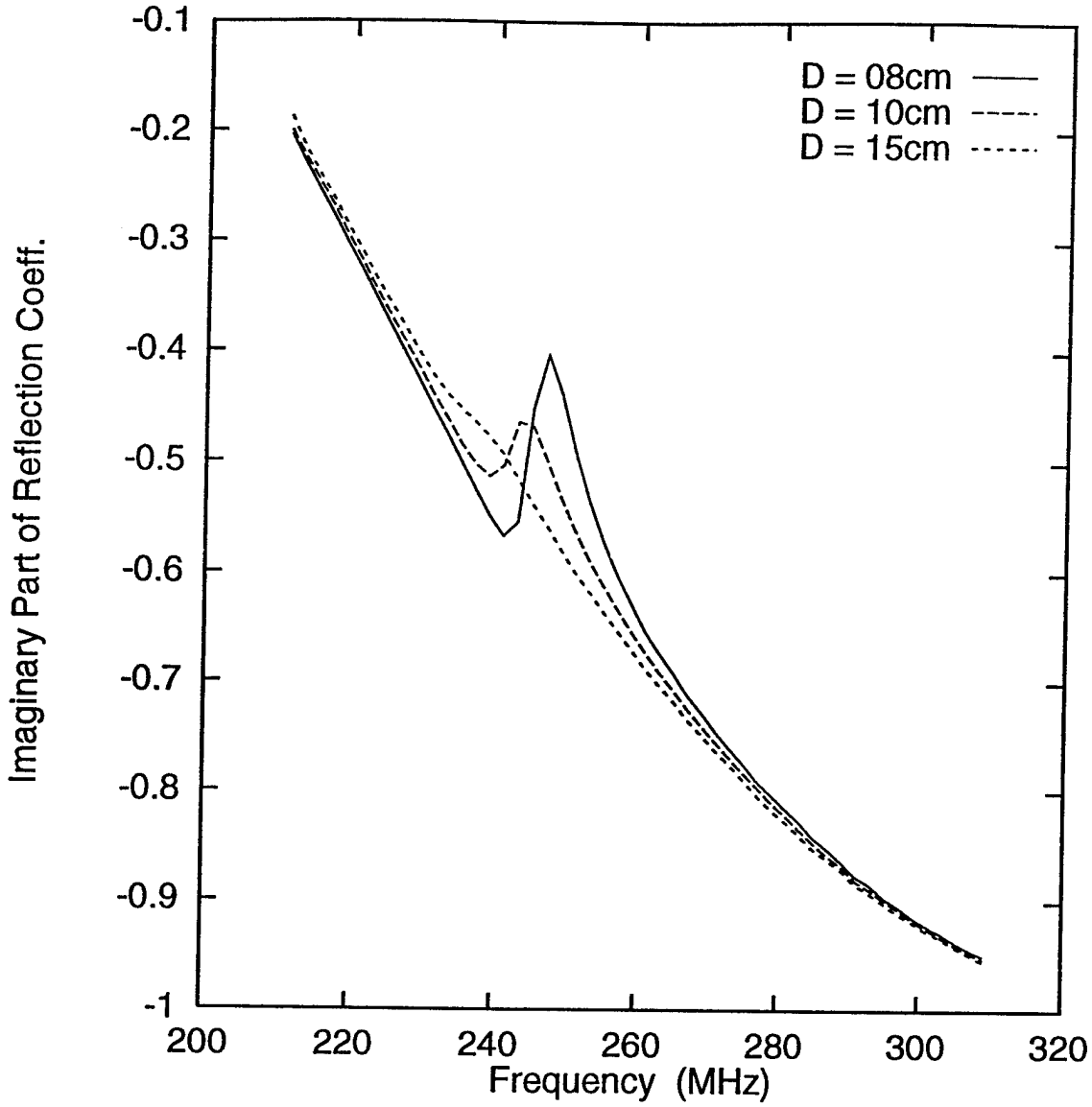

Figure 17. Imaginary part of S_{11} (Γ) for an untuned loop and target distances of D = 8, 10, and 15 cm for a 0.635 cm target thickness.

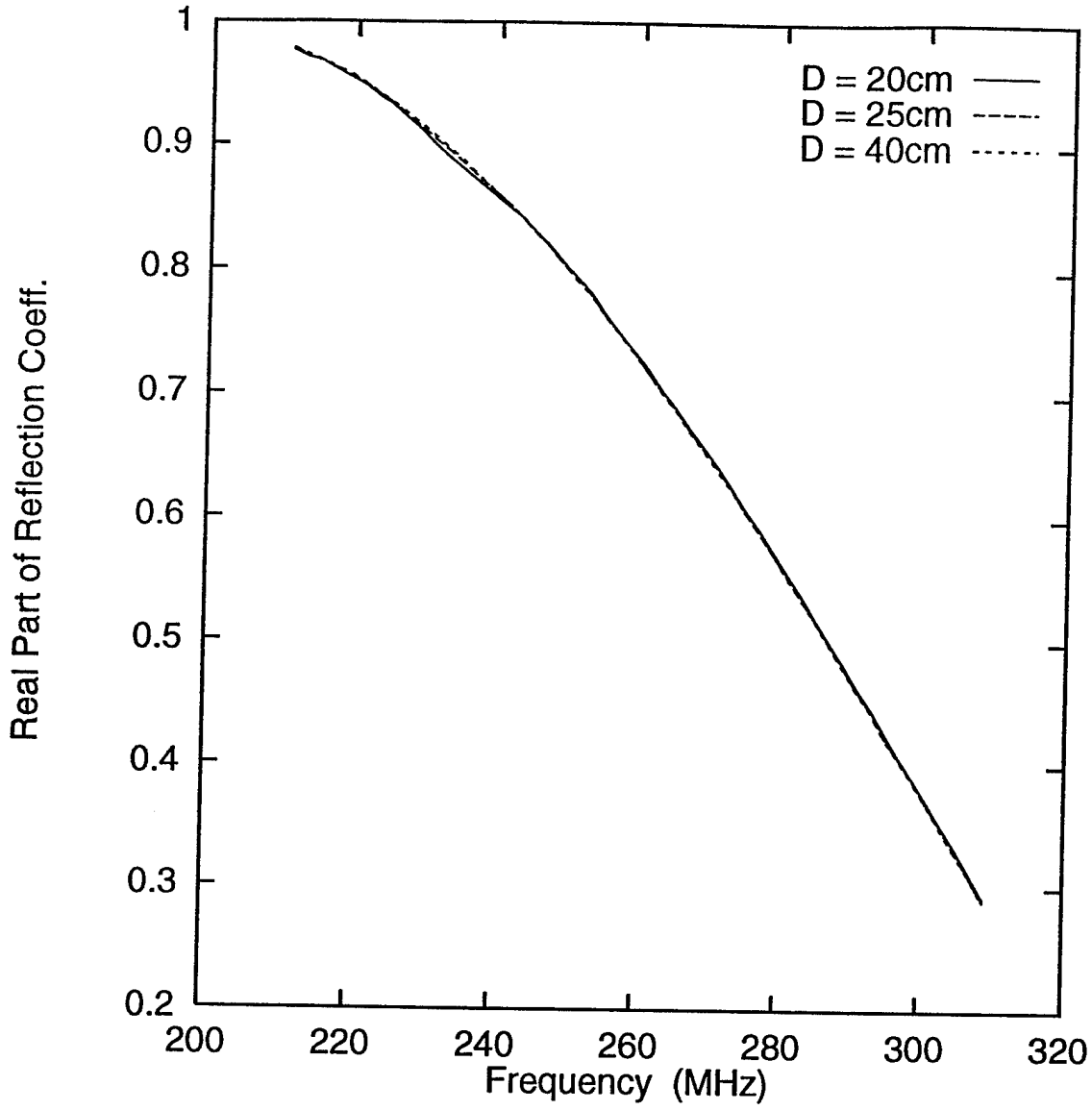

Figure 18. Real part of S_{11} (Γ) for an untuned loop and target distances of D = 20, 25, and 40 cm for a 0.635 cm target thickness.

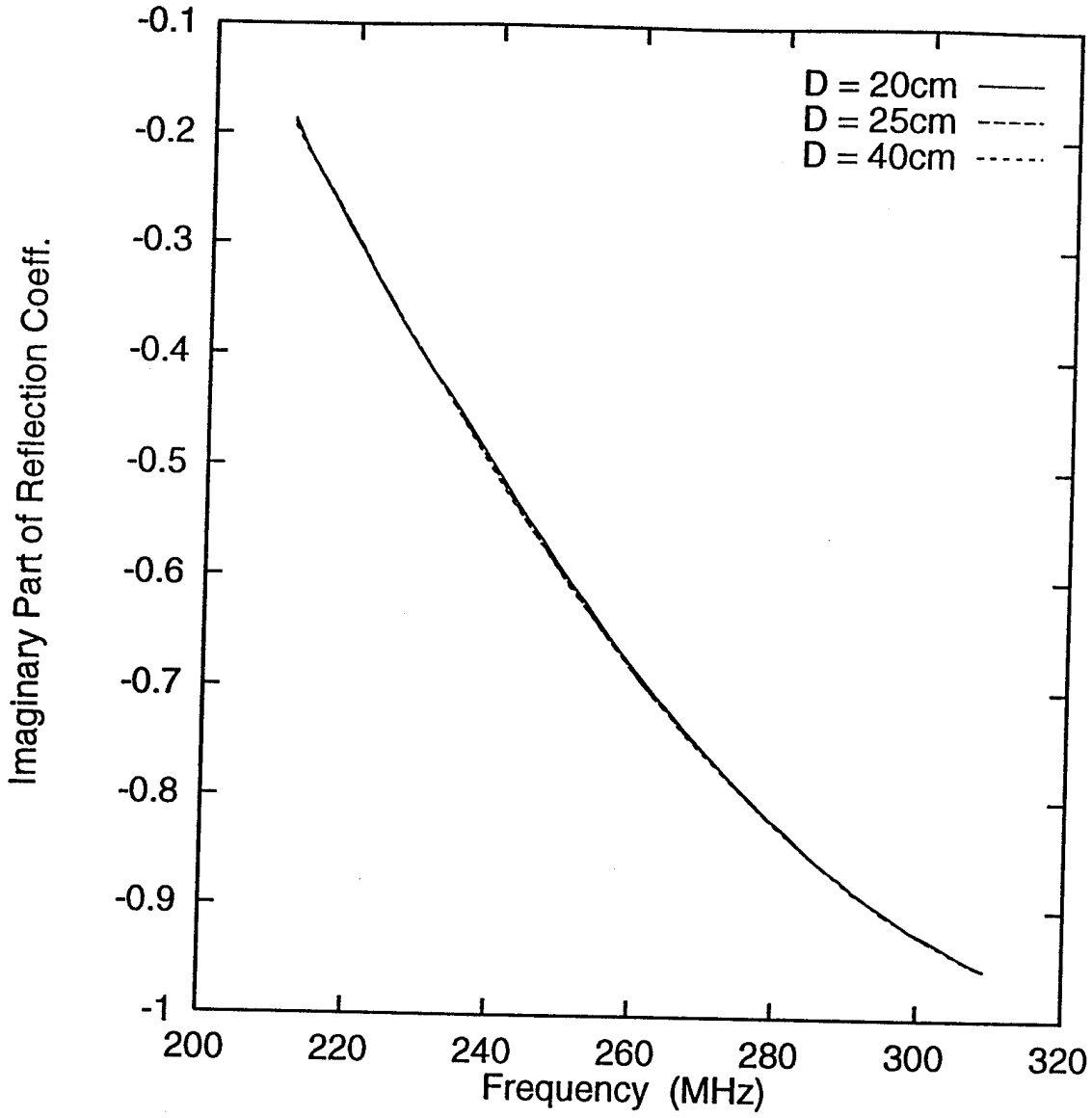

Figure 19. Imaginary part of S_{11} (Γ) for an untuned loop and target distance of D = 20, 25, and 40 cm for a 0.635 cm target thickness.

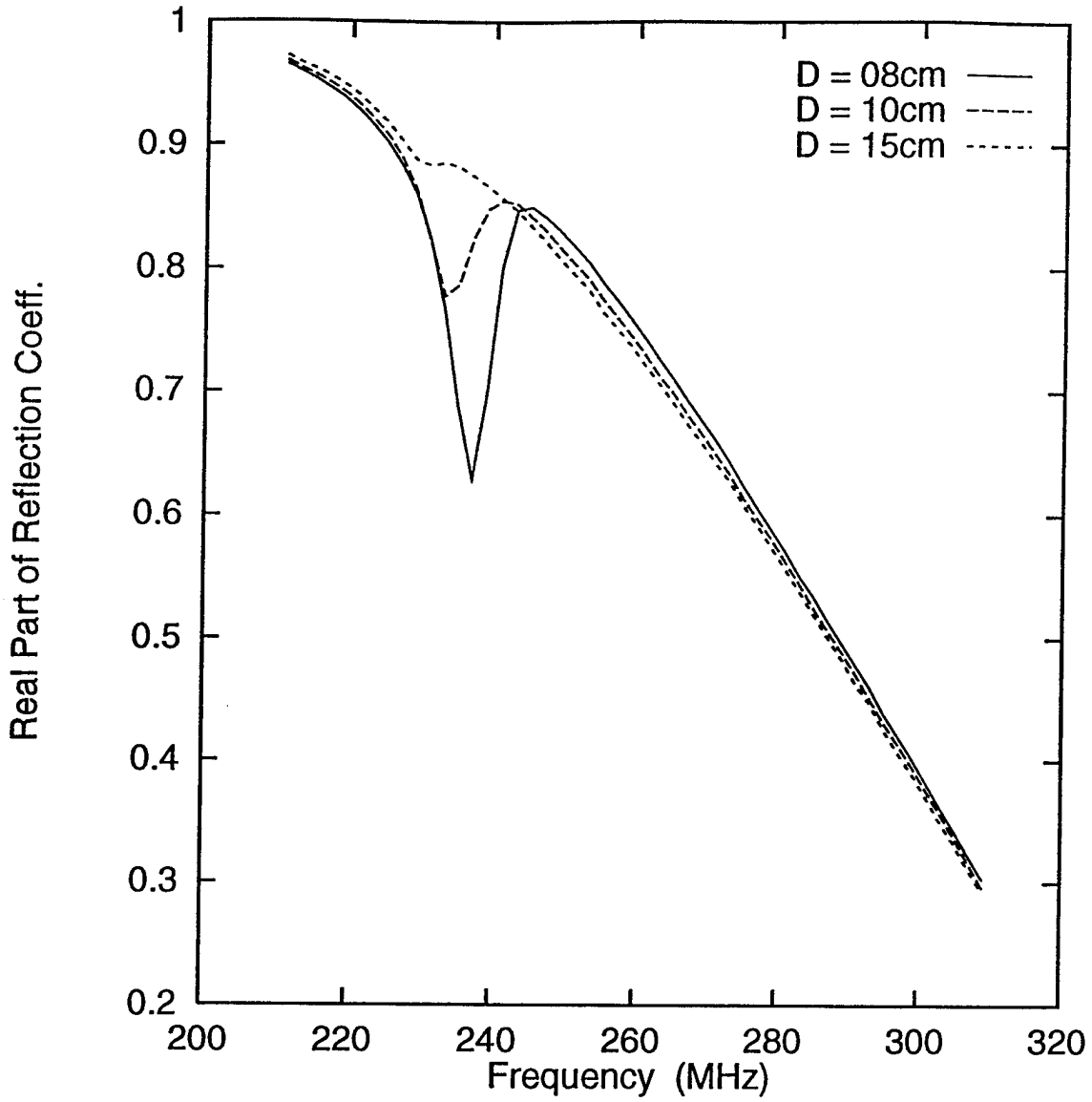

Figure 20. Real part of S_{11} (Γ) for an untuned loop and target distances of D = 8,10, and 15 cm for a 1.829 cm target thickness.

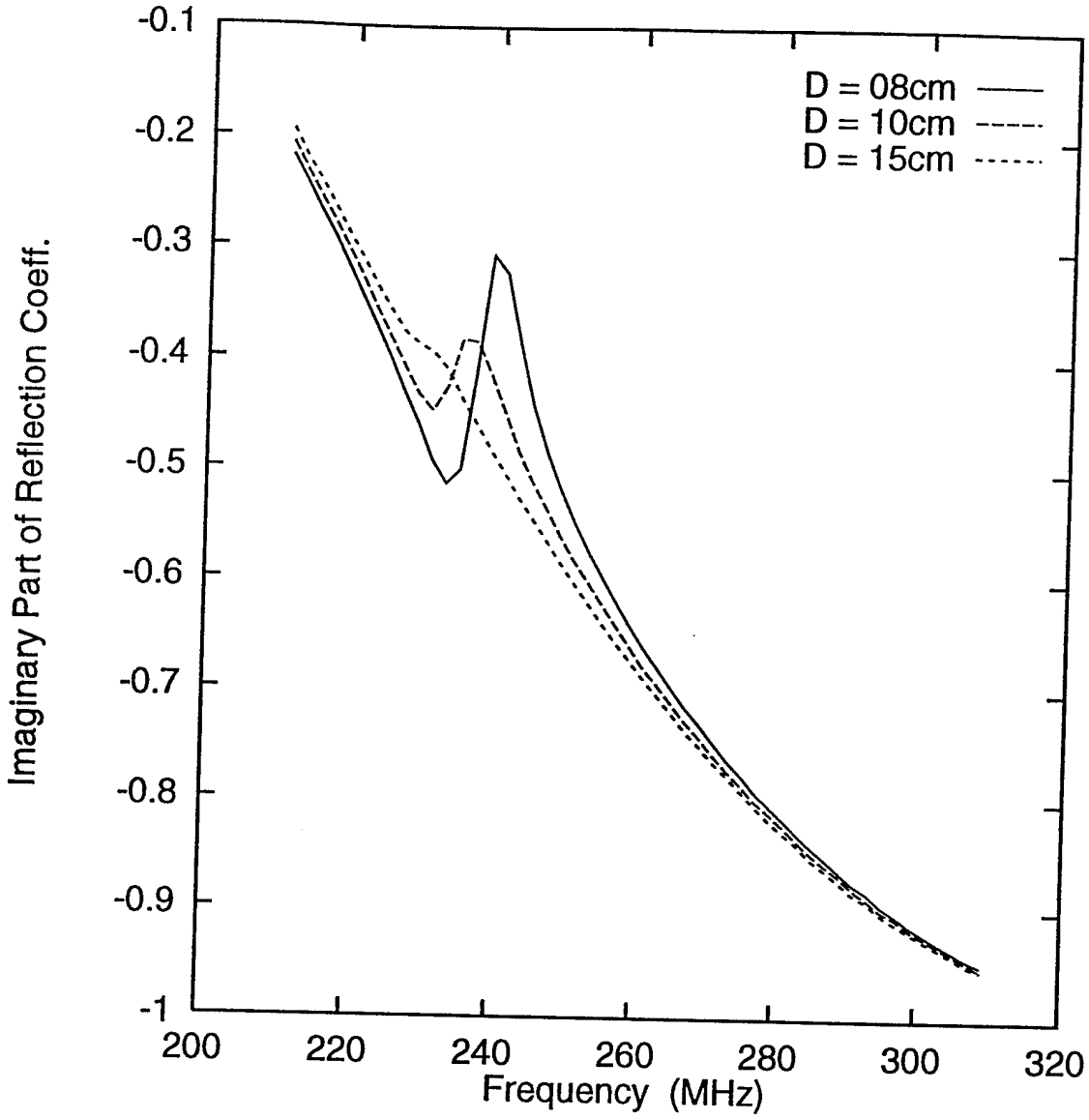

Figure 21. Imaginary part of S_{11} (Γ) for an untuned loop and target distances of D = 8,10, and 15 cm for a 1.829 cm target thickness.

larger influence on S_{11} as compared to the results for the small thickness target of Figs. 16 and 17, as would be expected intuitively for targets in the near field of the antenna.

Because of the limited distance where the loop-target coupling is visible in the measured data (i.e., where a difference between a target and no target case can be seen), two approaches were employed to increase the target distance where the coupling is visible. Both of these approaches increase the antenna loop current, the first by using a tuned loop and the second by simply increasing the power input to the antenna. To obtain a resonant antenna, a single stub tuned configuration was employed to obtain a no target resonance of approximately 250 MHz. A series of measurements were made using the HP8510B VNA for target distances of D= 8, 10, 15, 20, 25, 30, and 40 cm. The target coupling in the tuned cases introduced a decided frequency shift in the S_{11} curves for small target distances as shown in Figs. 22 through 25, and a small discernible difference at larger target distances. This indicates an increase in sensitivity of the target measurement using a tuned loop.

The increase of loop current using higher input power was accomplished using a Hewlett Packard HP8755 scalar network analyzer in conjunction with a 1 Watt RF power amplifier and the single stub tuned loop and ground plane. Phase information cannot be obtained with this configuration as shown in Fig. 26; however, the effect of coupling can be determined from the magnitude variation of S_{11} as a function of target distance. A narrowband plot of the magnitude of reflection coefficient for the single stub tuned loop with 1 Watt power input, as shown in Fig. 27, shows easily discernible shifts in the loop's resonance frequency for distances of at least 30 cm, as compared to the small changes observed for the reflection coefficient of the untuned loop as shown in Figs. 16 through 21. A wideband plot of $|S_{11}|$ data in Fig. 27 is given in Fig. 28. In Fig. 28, the apparent resonance point of each of the different target distances are manually offset so that the plotted magnitude can be easily determined. The apparent frequency of each resonance point (minimum) is thus not at the correct frequency, but the magnitude and the shape relative to the resonance frequency can be accurately determined. Figures 27 and 28 demonstrate that the assumption that higher loop current can used to extend the distance

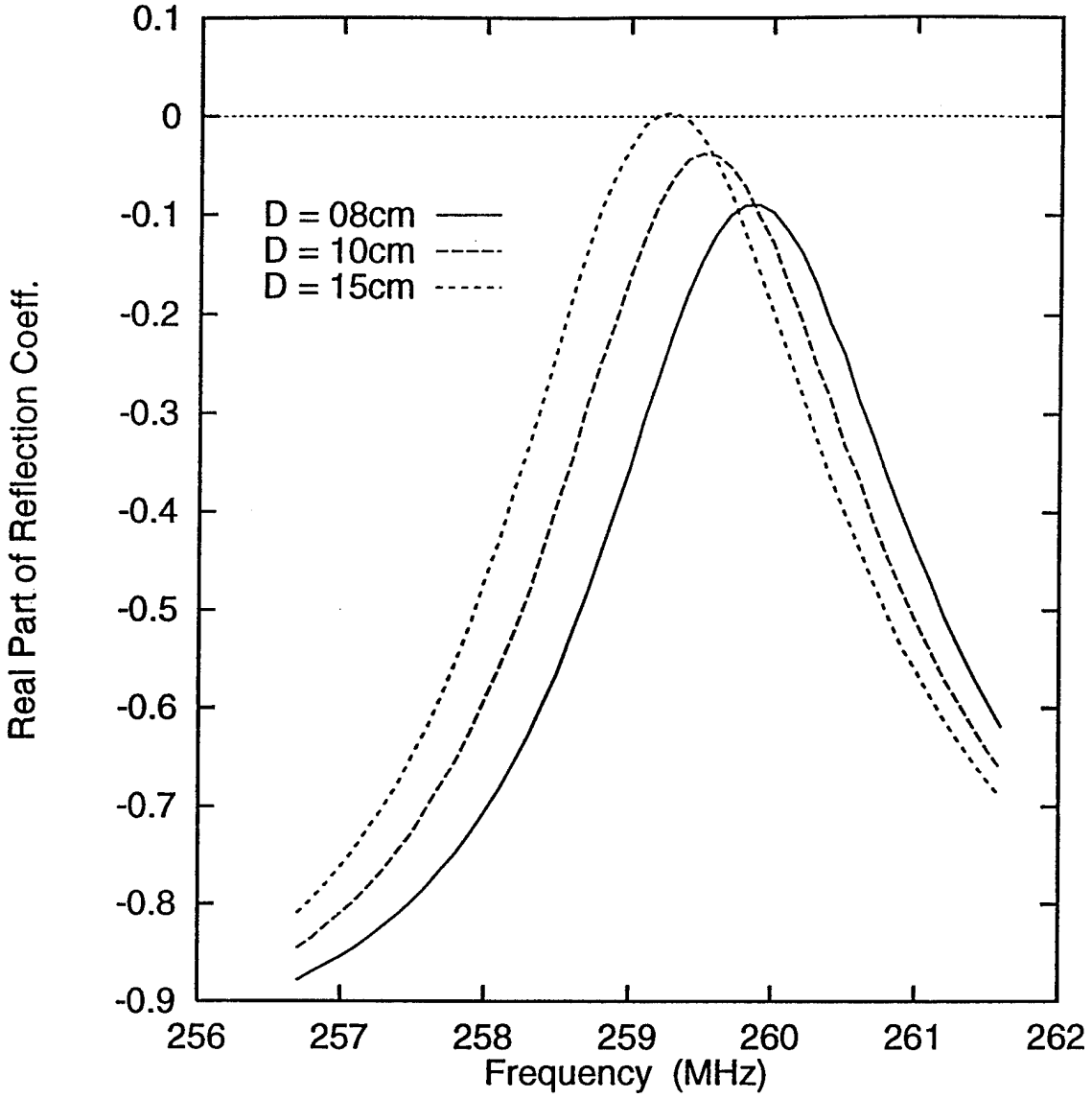

Figure 22. Real part of S_{11} (Γ) for a single stub tuned loop and target distances of 8, 10, and 15 cm for a 0.635 cm target thickness.

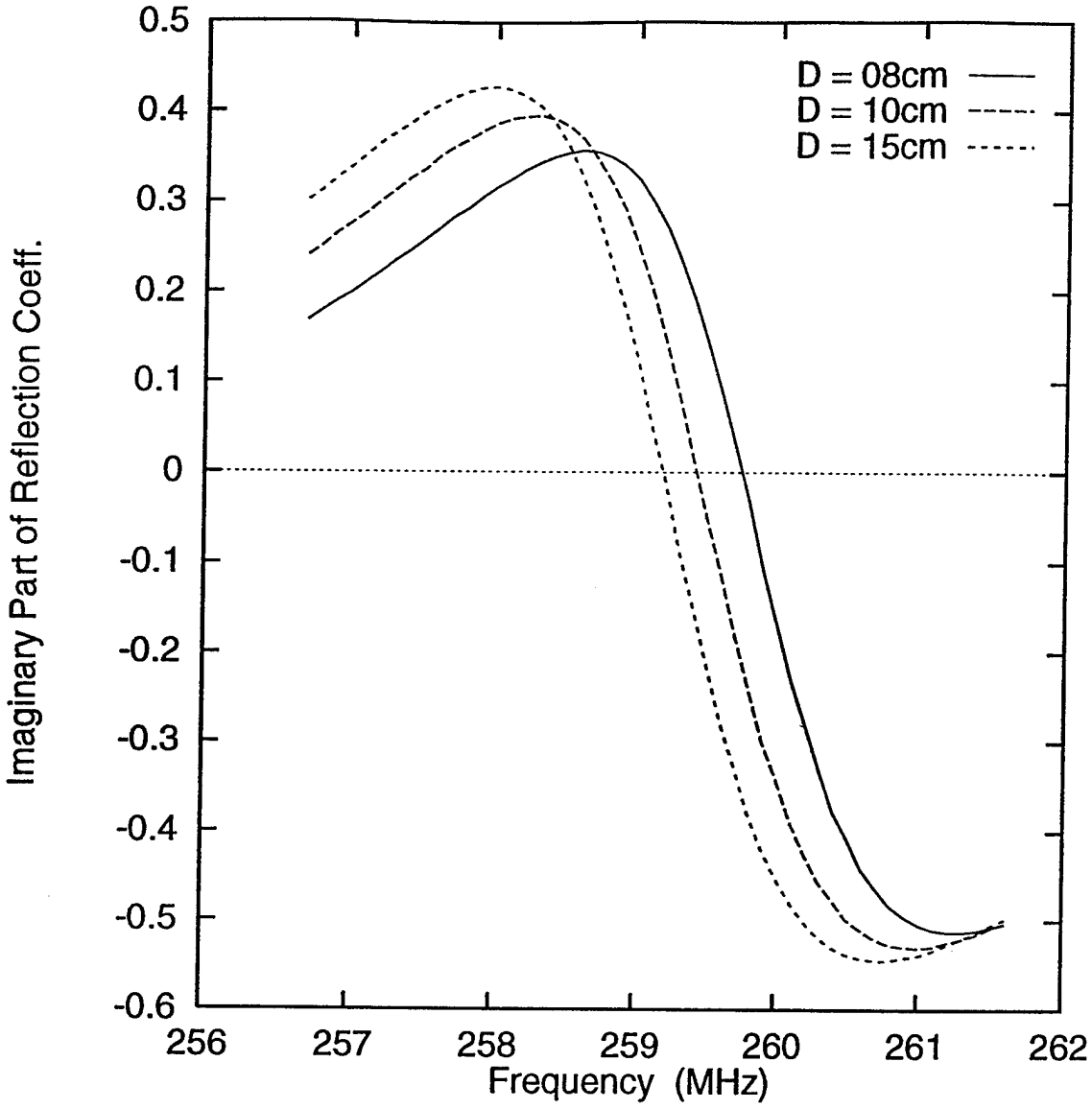

Figure 23. Real part of S_{11} (Γ) for a single stub tuned loop and target distances of 8, 10, and 15 cm for a 0.635 cm target thickness.

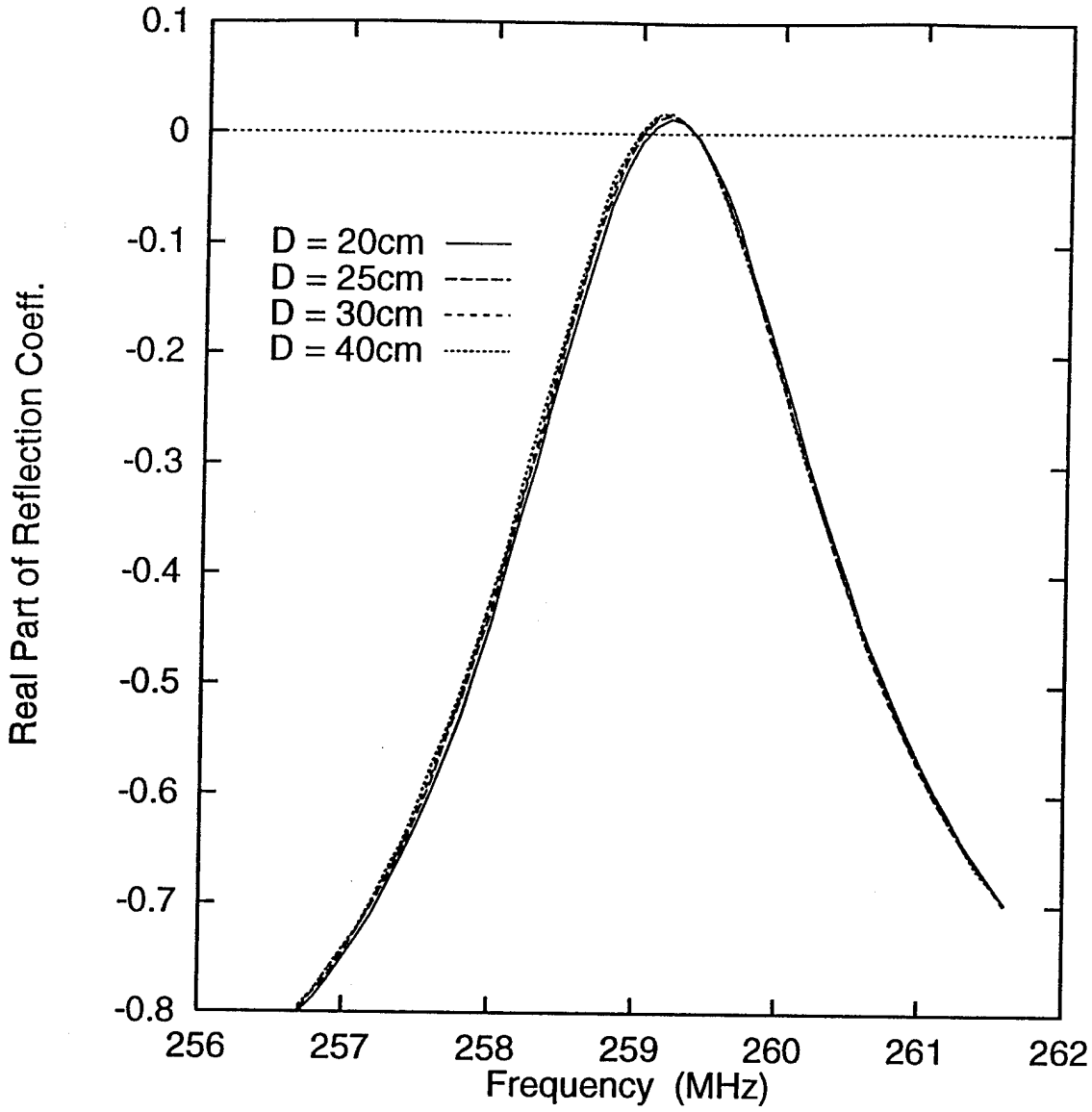

Figure 24. Real part of S_{11} (Γ) for a single stub tuned loop and target distances of 20, 25, 30 and 40 for a 0.635 cm target thickness.

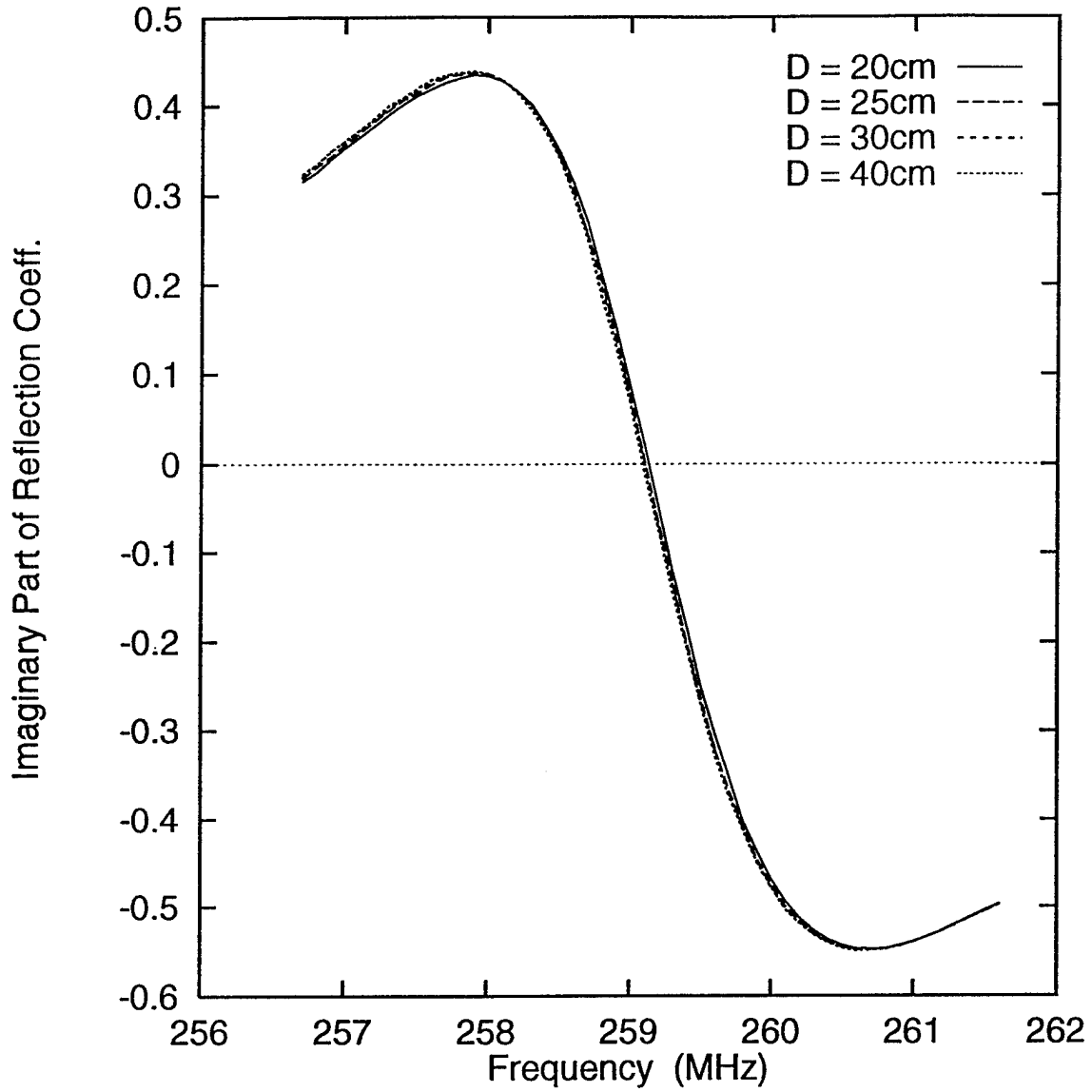

Figure 25. Imaginary part of S_{11} (Γ) for a single stub tuned loop and target distances of 20, 25, 30 and 40 cm for a 0.635 cm target thickness.

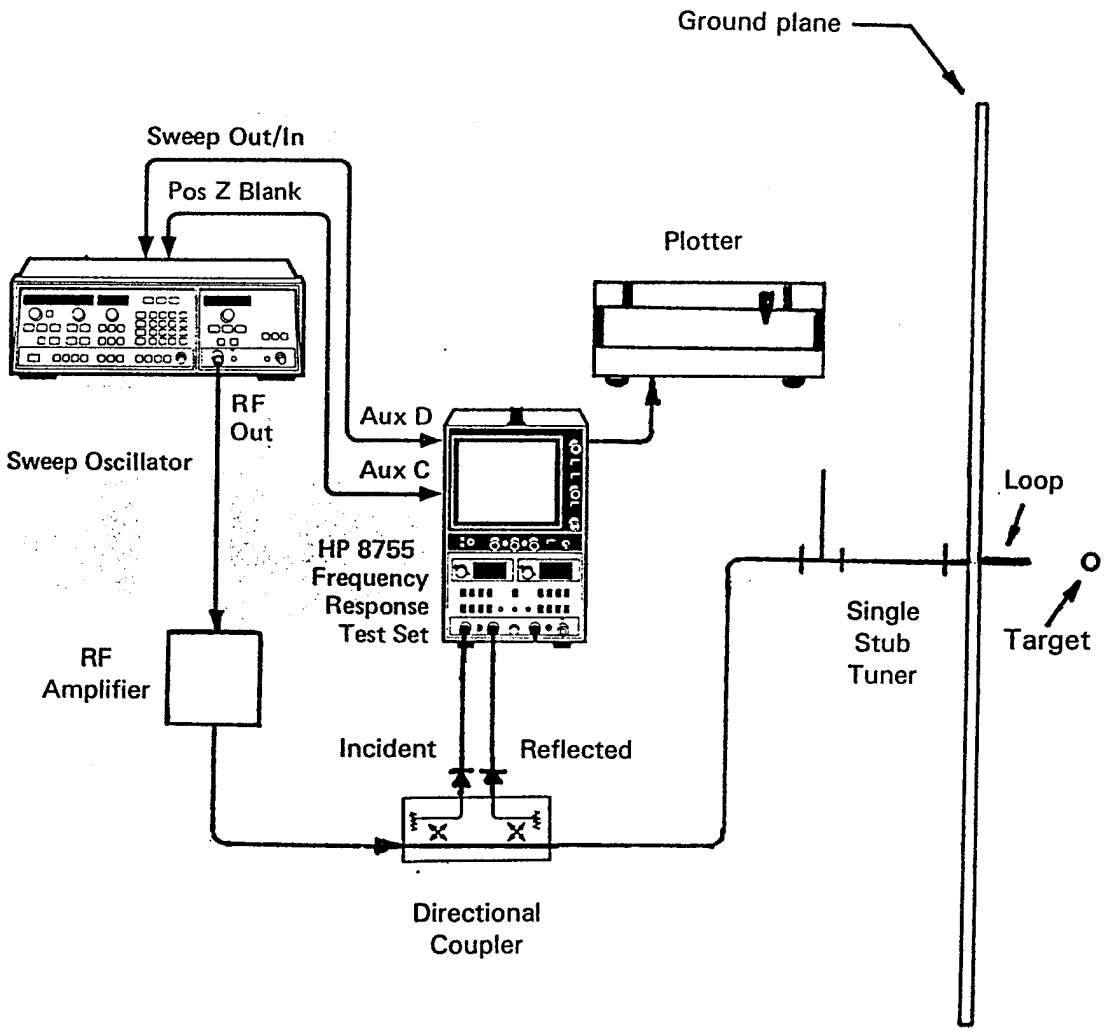

Figure 26. Measurement configuration for single stub tuned loop with high power input.

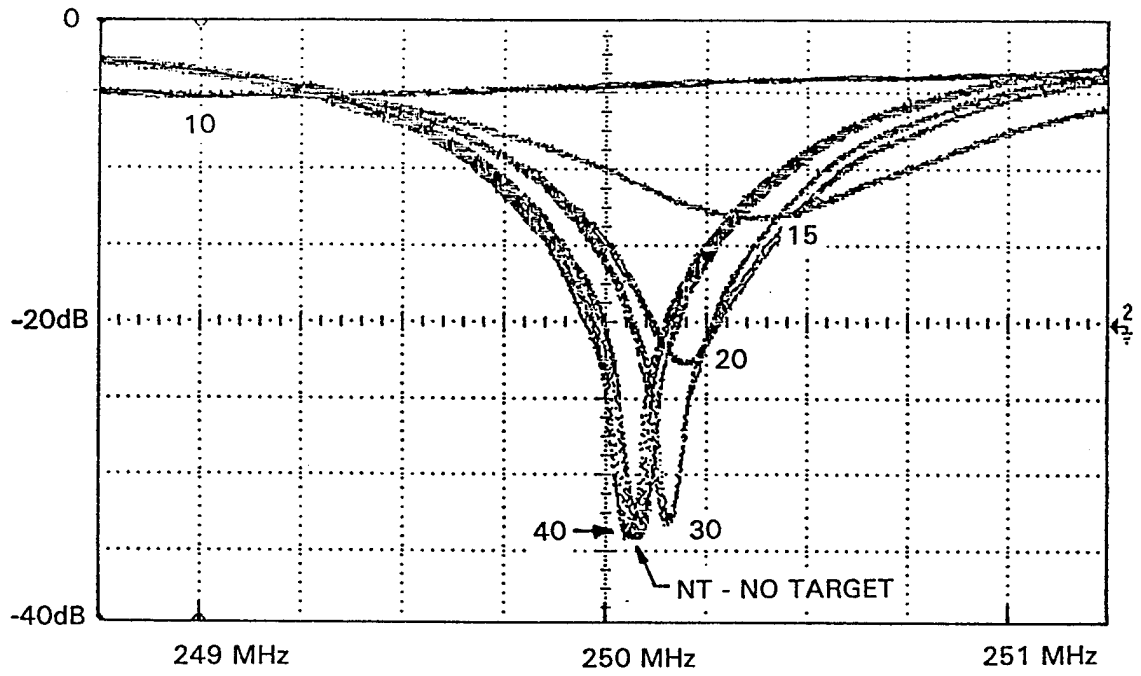

Figure 27. Magnitude of reflection coefficient for a loop antenna (single stub matched for no target) for target distances of 10, 15, 20, 30, and 40 cm. The target is 0.635 cm (1/4") tubing 56 cm in length.

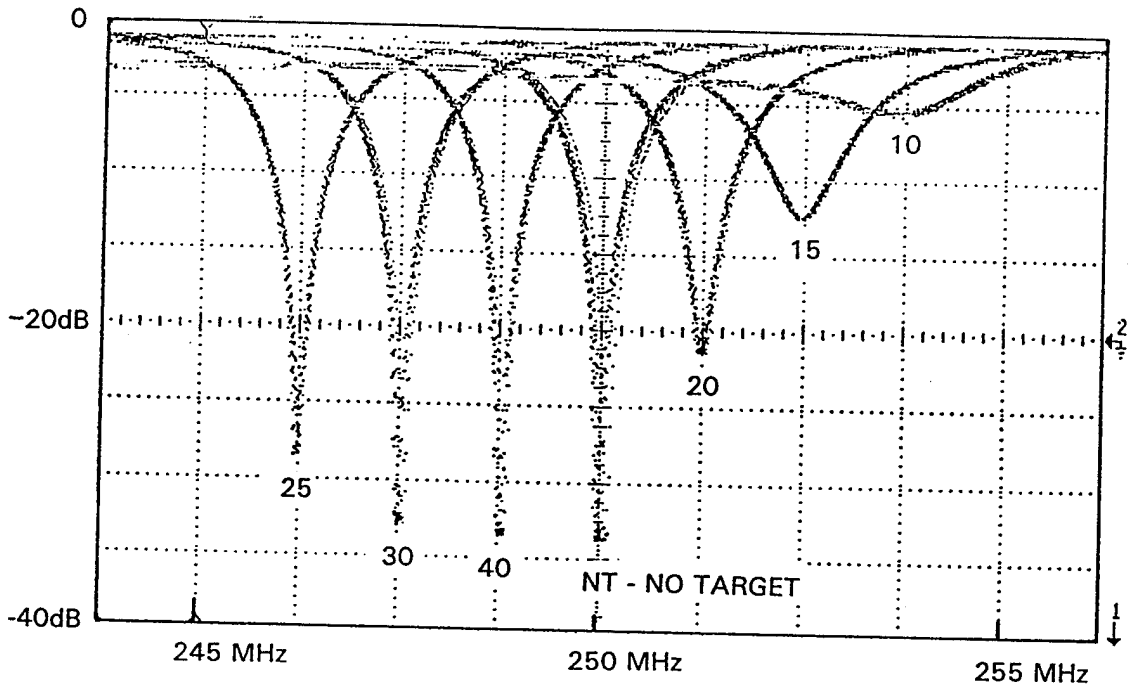

Figure 28. Magnitude of reflection coefficient for loop antenna (single stub matched for no target) for target distances of 10. 15, 20, 30, and 40 cm. The target is 0.635 cm (1/4") tubing 56 cm in length. Individual responses shifted of 1 division to facilitate minimum determination.

at which the target coupling can be measured has been demonstrated to be correct and that practical implementations of the technique are feasible.

In this study we have proposed that the antenna's input admittance, Y, be measured and used to calculate the target sensing function ($T_s = 1 - |Y/Y_i|$) and that the target sensing function versus frequency data be used to determine the presence and identity of the buried target. The target sensing function is zero when no target is present and when a target is present, it tends to exhibit a maximum or minimum at a frequency at or near the targets fundamental resonant frequency (for targets in the near field of the antenna). Computed and measured results for the target sensing function are presented in Fig. 29 for a target separation distance of 15 cm and a target thickness of 0.635 cm and target length of 56 cm. The results presented in Fig. 29 indicate a very good agreement between the numerical and measured data especially at frequencies above the target's resonant frequency. The comparison of computer simulation generated to the measured results presented in Fig. 29 verifies the antenna and target model used in this study and supports the use of the target sensing function for the proposed ground coupled radar system.

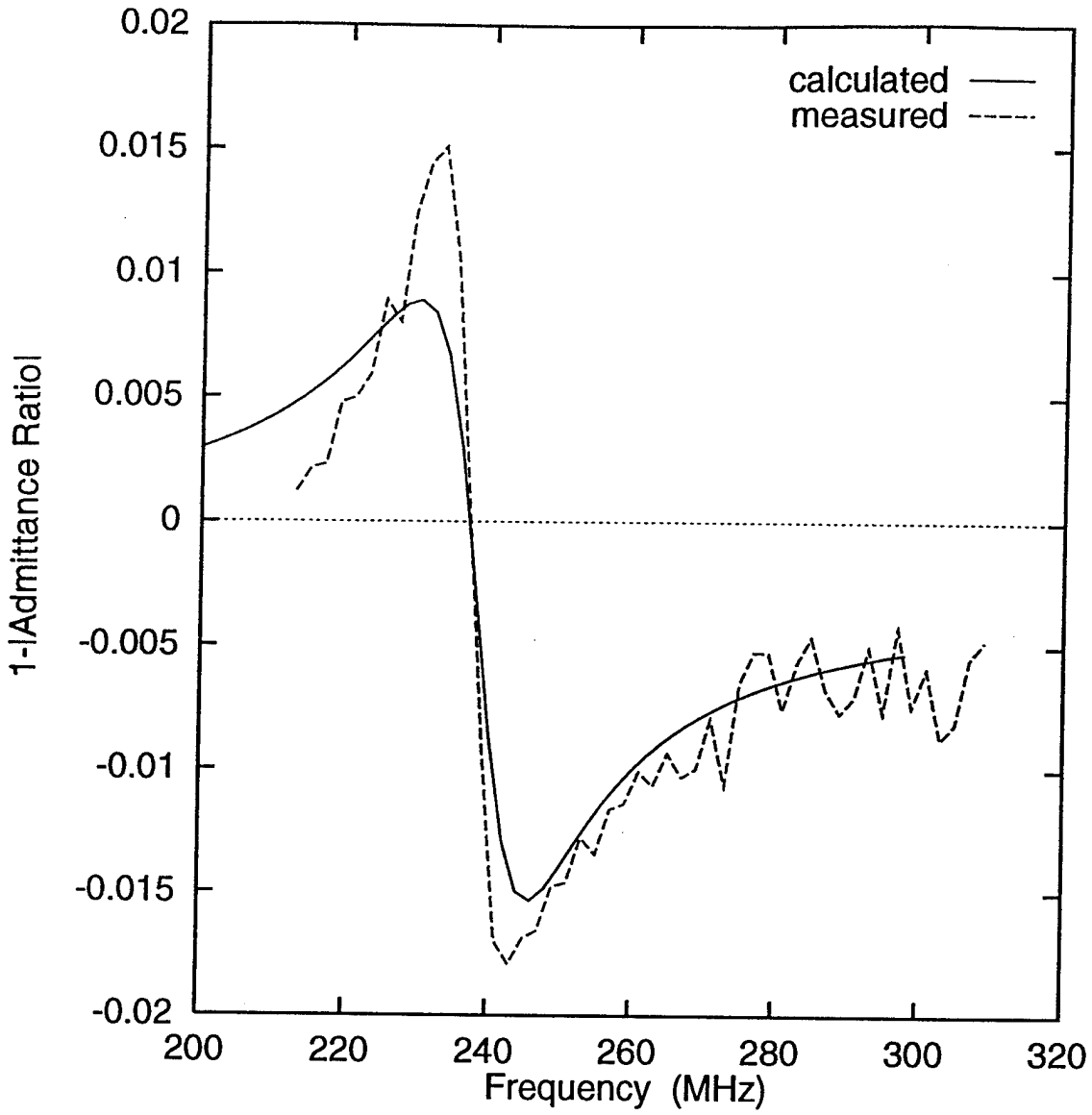

Figure 29. One minus the magnitude of the ratio of the loop antenna input admittance with a target present to the input admittance of the isolated loop versus frequency. The center of the wire target is 15 cm from the center of the loop and the loop is untuned. The target is 0.635 cm (1/4") tubing 56 cm in length. Both measured and calculated results are given.

Conclusions and Areas for Future Study

Both the calculated and measured results presented in the previous section are encouraging and we believe they indicate that additional investigation is warranted. These initial results indicate several areas which need careful investigation. Several of these areas must be investigated before the feasibility of the method investigated here is really known. In this section we discuss these areas.

Target Q factor

The target Q factor affects both the depth and frequency width of the admittance ratio null. The depth increases with increasing Q while the width decreases with increasing Q. A high target Q factor is therefore desirable for target detection and identification. For cylinders, the Q factor is a decreasing function of the cylinder length to diameter ratio. For a PEC cylinder, the maximum value of Q occurs in the thin wire case for which the Q value is 5. The fundamental resonant frequency and Q factor of an isolated 60 cm long PEC cylinder with a 1 cm diameter were determined using a computational code which is specific to axisymmetric objects [9, 10]. The fundamental resonant frequency and Q factor of the wire target are 225 MHz and 4.94, respectively.

For an unexploded shell, a realistic value of the length to maximum-diameter ratio is around 6. For a PEC cylinder with length 60 cm and diameter 10 cm, the Q factor is around 2. This Q factor may be too low for the proposed method to work because the resonant effect is not sufficiently distinct to observe. However, the Q factor is a strong function of the target's constitutive parameters. Results calculated assuming PEC material are very accurate for non-magnetic metals like aluminum. Our initial calculations indicate that for magnetic materials like steel, the Q factor value is greatly increased compared to the PEC case. Using a surface impedance approximation in our computational code for axisymmetric targets, we have an tentative Q factor estimate of 18 for a steel cylinder with length 60 cm and diameter 10 cm, assuming $\mu_r = 50$, $\sigma = 10^7$ S/m, as in [11]. (The work in [11] is for extremely low frequencies.) Note that this estimate of the Q factor has not

been verified by measurements and that the Q factor appears to be a very strong function of the relative permeability of the shell.

The determination of shell's actual Q factor when buried in the earth is an important part of future research. Note that an approximate analytical method for calculating the buried shell's resonant frequency and Q factor from the free-space values is presented in [12]. The analytical method presented in [12] has not yet been carefully studied by the authors.

Signal Dependent Noise

Having a sufficiently high Q factor for all shells in the range insures only that the shells have distinct enough responses to be differentiated from one another in the absence of signal independent and signal dependent noise.

Signal independent noise (such as thermal noise) can be reduced using standard methods and signal power can be increased so that the signal power to independent-noise power ratio can be made as large as necessary. As a result, the detection of buried shells is not an issue of independent noise but rather of signal dependent noise. An example of signal dependent noise familiar to a radar specialist is radar clutter. In detection and identification based on the swept frequency target sensing function, signal dependent noise comes from the variation of the isolated antenna admittance as the antenna is moved across the surface of the former artillery range. Evaluation of the signal dependent noise via measurements and numerical methods is a critical component of future development work.

Measurement Hardware

To simplify the measurement process for this initial investigation, an electrically-small loop antenna was used. While this antenna has its merits, it is may not be optimal for buried target detection and identification because of low sensitivity. By sensitive, we mean the maximum deviation of the target sensing function versus frequency for a particular target at a fixed distance from the antenna.

Future investigations must include the development of an antenna which maintains the simple loop's merits (good coupling to the soil via a primarily magnetic near field and the ability to work without touching the soil) but is more sensitive to the target's presence. Antenna designs that we feel merit investigation are shielded loops, arrays of loops, and electrically large loops with lumped tuning spatially distributed around the loop. In particular, this last option seems promising. The use of a small loop (relative to the wavelength) in this work was motivated by a desire to maintain a relative constant current around the loop (as illustrated in Fig. 3). Because antenna tuning was demonstrated to improve the system sensitivity by approximately two orders of magnitude, use of antenna tuning is strongly indicated in future development work. Note that, increasing the radius of the antenna loop without taking steps to maintain a constant current around the loop will not increase the sensitivity of the system. (The proceeding statement has been verified by computational studies using NEC-4). By distributing the tuning elements around the antenna loop, we feel that a relatively constant current can be maintained around a larger antenna loop. With a constant current distribution, the additional area of the loop will then increase the antenna's sensitivity.

As with the antenna, additional research and development work is needed to design a specialized network analyzer measurement system which improves the sensitivity of the ground coupling radar system. All but one of the measured results presented here were obtained using a standard laboratory network analyzer. Because the network analyzer is of general design and has limited output power, it is hardly optimal for making ground coupling radar measurements. Figures 27 and 28 are the result of our initial attempt at constructing a more sensitive measurement system. The preliminary results presented in Figs. 27 and 28 illustrate that use of a higher antenna current than can be obtained with a standard laboratory network analyzer results in increased sensitivity of the measurement system. Many other hardware improvements are possible to increase the sensitivity of the ground coupling radar system.

Model Based Target Identification Algorithm

Both the hardware design and the physics of ground coupling are important aspects of the buried target detection and identification problem. These two were investigated in this initial study. Another aspect of the buried target detection and identification problem answers the question of what one does with the measured signal so that the target can be detected and identified. This is the signal processing aspect of the radar system. Without a simultaneous investigation of the measurement hardware aspect, the ground coupling aspect, and the signal processing aspect, the performance of the proposed ground coupling radar system cannot be determined.

Signal processing was not investigated in this initial study. In future work, the signal processing aspect of the detection and identification problem must be investigated. Other investigators [1-4] have focused of the extraction or use of the SEM poles of the buried target to detect and identify the target. By focusing on a single coupling (scattering) mechanism to detect and identify the target, these methods "throw away" other information in the signal which can be used to detect and identify the target. In many cases there is more "information" in the "thrown away" part of the signal than is in the part of the signal which results from the response of the SEM poles.

This fact has received much attention recently in the area of radar target identification of aircraft. A particularly promising target detection and identification algorithm has been developed for the U.S. Army by Dr. Larry Bretthorst of Washington University [13]. This model based target ID algorithm was developed using Bayesion methods. The authors are familiar with this technique and feel that this type of processing has great promise for providing robust buried target detection and identification.

Conclusion

This initial study provided verification of the proposed ground coupling radar concept. In addition, it started the investigators (Professors and Graduate Students) down the road to a more complete understanding of the various aspects of the ground coupling radar problem. The primary contributions of this work are as follows:

1. The development of the target sensing function to isolate the effect of the target from the measured (or calculated) antenna input admittance.
2. The introduction of antenna tuning to increase the sensitivity of the ground coupled radar system.
3. The experimental verification that increased antenna current achieved either through antenna tuning or increased transmitter power, results in increased sensitivity of the ground coupling radar system.

Due to the complex nature of detection and identification problems, no initial study can answer the question of whether the proposed method is ultimately useful for the detection and identification of buried shells. This study does, however, make clear what aspects of the problem must be investigated to answer this question. As previously stated, without a simultaneous investigation of the measurement hardware aspect, the ground coupling aspect, and the signal processing aspect, the performance of the proposed ground coupling radar system cannot be determined.

References

[1] L.C. Chan, D.L. Moffatt, and L. Peters, Jr., "A characterization of subsurface radar targets," *Proceedings of the IEEE*, vol. 67, no. 7, pp. 991-1000, July 1979.

[2] Y. Hua and T.K. Sarkar,"T-pulse for exciting single modes of radar targets," *Ultra Wideband Radar: Proceedings of the First Los Alamos Symposium*, Editor: Bruce Noel, CRC press, pp. 39-53, 1991.

[3] L. Peters, Jr., J. J Daniels, and J. D. Young, "Ground penetration radar as a subsurface environmental sensing tool," *Proceedings of the IEEE*, vol. 82, no. 12, pp. 1802-1822, December 1994.

[4] C. Chen, L. Peters, Jr., and W. D. Burnside, "Ground penetration radar target classification via complex natural resonances," *1995 IEEE AP-S International Symposium Digest*, vol. 3, pp. 1586-1589, June 1995.

[5] G. J. Burke, *Numerical Electromagnetics Code - NEC-4 Method of Moments Part I: User Manual, Part II; Program Description - Theory*, Lawrence Livermore National Laboratory Report Number UCRL-MA-109338, January 1992.

[6] J. Chen, A. A. Kishk, and A. W. Glisson, "MPIE for a conducting sheet penetrating a multilayer medium," 1994 IEEE International Antennas and Propagation Society Symposium Digest, vol. 2, pp. 1346-1349, Seattle, WA, June 1994.

[7] W. Zheng, *Wire antennas above and protruding through and air/lossy medium interface*, University of Mississippi Dissertation, May 1995.

[8] W. Zheng, A. A. Kishk, and C. E. Smith, "A model for cylindrical antennas in a multilayer medium," *Proceedings of the 27th Southeastern Symposium on System Theory*, March 12-14, 1995 at Mississippi State University.

[9] A. A. Kishk, "Electromagnetic Scattering from Composite Objects Using a Mixture of Exact and Impedance Boundary Conditions," *IEEE Trans. Antennas Propagation*, vol. AP-39, no.6, pp. 826-833, June, 1991.

[10] A. A. Kishk, A. W. Glisson, and D. Kajfez, "Computed resonant frequency and far fields of isolated dielectric discs," *1993 IEEE AP-S International Symposium Digest*, vol. 1, pp. 408-411, 1993.

[11] A. R. Sebak, L. Shafi, and Y. Das, "Near-zone fields scattered by three-dimensional highly conducting permeable objects in the field of an arbitrary loop," *IEEE Transactions on Geoscience and Remote Sensing*, vol. 29, no. 1, pp. 9-15, January 1991.

[12] C. E. Baum, The SEM Representation of scattering from perfectly conduction targets in simple lossy media," Phillips Laboratory Interaction Note 492, April 1993.

[13] Larry Bretthorst, "Radar Target Identification in the Frequency Domain," Final Report for the U.S. Army Research Office, Contract Number DAAL03-91-0034, Task Control Number 94-206, Delivery Order Number 1254, December 1995.

Contractually Required Information

List of Participants

Paul M. Goggans, Associate Professor
Charles E. Smith, Professor and Chair
Jeffrey Pursel, M. S. Graduate Assistant
Wenhai Yang, M. S. Graduate Assistant

List of Publications

Lloyd S. Riggs and Paul M. Goggans, "Using the quasi-magnetostatic response for target identification of buried objects," to be presented at The 10th Annual International AeroSense Symposium, April 9, 1996 in Orlando, FL.

Report of Inventions

There were no inventions declared within this project.